How DUXC-family transcription factors influence immune signaling: implications for muscular dystrophy, cancer, and early development

Amy Elizabeth Spens

A dissertation

submitted in partial fulfillment of the

requirements for the degree of

Doctor of Philosophy

University of Washington

2022

Reading Committee:

Stephen J Tapscott, Chair

Michael Gale Jr.

Robert Bradley

Program Authorized to Offer Degree:

Molecular and Cellular Biology

University of Washington

Abstract

How DUXC-family transcription factors influence immune signaling: implications for muscular dystrophy, cancer, and early development

Amy Elizabeth Spens

Chair of the Supervisory Committee:

Stephen J Tapscott

Department of Neurology

DUXC-family transcription factors are endogenously expressed at the cleavage stage of development in placental mammals and help drive an initial burst of zygotic gene transcription. However, misexpression of the human ortholog DUX4 in adult skeletal muscle is the causative factor in Facioscapulohumeral muscular dystrophy (FSHD). Additionally, expression of DUX4 in solid cancers leads to downregulation of MHC-I antigen presentation machinery and is correlated with immune evasion. Here, I show that DUX4 also suppresses the transcriptional response to Type-II interferon gamma (IFNγ), Type-I interferon beta (IFNβ), double stranded (ds)RNA, and dsDNA treatments. A transcriptionally silent C-terminal portion of the DUX4 protein interacts with activated forms of STAT1, reduces its binding at interferon stimulated gene (ISG) promoters, and destabilizes assembly of the transcriptional complex, thus preventing

ISG upregulation. Transcriptional suppression of ISGs requires conserved (L)LxxL(L) motifs in the carboxyterminal region of DUX4 and phosphorylation of STAT1 Y701 enhances interaction with DUX4. Consistent with these findings, expression of endogenous DUX4 in FSHD muscle cells and the CIC-DUX4 fusion containing the DUX4 CTD in a sarcoma cell line inhibit IFNγ-induction of interferon-stimulated genes (ISGs). Mouse Dux similarly interacted with STAT1 and suppressed IFNγ induction of ISGs. These findings identify an evolved role of the DUXC family in modulating immune signaling pathways with implications for development, cancers, and FSHD.

TABLE OF CONTENTS:

List of Figures

ACKNOWLEDGEMENTS

Intentionally left blank for now. ☺

Chapter 1: INTRODUCTION

1.1 Roles for immune signaling in health and development

While people most commonly think of the immune system as defending against viruses, bacteria, and other pathogens, both innate and adaptive immune cells and immune signaling pathways play crucial roles in broader tissue function and homeostatis, health, and development. For instance, multiple components of the innate and adaptive immune systems play roles in the regeneration of skeletal muscle following injury. Damage to muscle cells activates the innate immune system, including complement, and results in activation of local mast cells and neutrophils [1-3] that eventually attract macrophages and T cells, leading to accumulation of cytokines such as TNF-α, IFNγ, and IL-1β [4-7], the combination of which is sufficient to stimulate proliferation of muscle stem cells and muscle regeneration *in vivo* [8, 9]. The immune system also plays a critical role in surveying tissues to detect and clear mutated or pre-cancerous cells before they can develop further. Cytotoxic T cells recognize peptides loaded onto MHC Class I antigen presentation machinery, so tumors that downregulate or mutate MHC, or cancer cells that have reduced responsiveness to IFNγ, can efficiently evade immune surveillance and develop resistance to checkpoint blockade immunotherapies [10-12]. Finally, regulation and appropriate suppression of the maternal immune response is critical for fetal tolerance, particularly in placental mammals. Embryonic implantation and the invasion of the embryo-derived portion of the placenta into maternal tissues represents a unique immunological struggle. In human placenta, cell-surface expression of MHC class I is restricted to specific subtypes [13-16], maternal CD4+ T helper 1 cells are downregulated [17-19], and cytokine responses are abrogated through downregulation of NF-kB [17, 20, 21]. These are just three examples of the roles the immune system plays in guiding tissue health and development.

1.2 DUXC-family genes in development and disease

The DUXC-family of transcription factors is unique to placental mammals. This family is characterized by the presence of two N-terminal homeobox DNA-binding domains and a highly conserved C-terminal domain containing two (L)LxxL(L) motifs. This C-terminal domain acts as the transcriptional activation domain, recruiting coactivators CBP and p300 that [22-24]. While putative genes encoding DUXC family members have been identified in multiple species, most functional studies of DUXC proteins have focused on Human DUX4, mouse Dux, and canine DUXC [25-27]. Human DUX4, murine Dux, and canine DUXC are thought to have arisen from a retrotransposition of the more ancestral DUXC, based on the lack of introns and the similarity of the homeodomain sequences [26, 28, 29]. Additionally, these transcription factors share a conserved role in activating the early embryonic gene signature that drives a full 2C-like state, including reactivation of endogenous retroviruses (ERVs), elongation of telomeres, derepression of heterochromatin, and chromocenter formation [25, 26, 29].

Misexpression of human DUX4 in adult skeletal muscle is the causative factor in Facioscapulohumeral muscular dystrophy (FSHD), the third most common form of muscular dystrophy [30]. The DUX4 gene exists in a tandem array of 3.3kb repeat units, termed the D4Z4, in the subtelomeres of chromosomes 4q and 10q [31, 32]. In unaffected individuals, the tandem array on chromosome 4q contains 11 to 100 copies of the *DUX4* gene. There are two well-documented forms of FSHD, both autosomally inherited: FSHD1, a dominant disease caused by contraction of the repeats of the D4Z4 on chromosome 4q to fewer than 10 units [33, 34], and FSHD2, a recessive disorder caused by mutation to the genes that repress *DUX4* expression such as structural maintenance of chromosomes flexible hinge domain-containing 1 (*SMCHD1*) and DNA methyltransferase 3B (*DNMT3B*) [35-37]. While FSHD1 is more common (thought to

represent 95% of cases), both FSHD1 and FSHD2 result in the demethylation and subsequent derepression of the D4Z4 and subsequent expression of *DUX4* and present with near-indistinguishable clinical symptoms [38]. Both types of FSHD are characterized by progressive weakening of the muscles of the face, upper arms, and shoulders, but generally do not affect cardiac muscle and rarely affects the respiratory system. Muscular weakness typically does not appear until young adulthood, with some patients not showing symptoms until much later in life; however, there are instances of individuals showing symptoms from infancy [30, 39]. Biopsies of FSHD muscles reveal cellular necrosis, centralized nuclei, variable fiber size, and immune cell infiltration, and muscles positive for T2-STIR by MRI have a higher probability of detectable *DUX4* expression than MRI-normal muscles [30, 40-43].

1.3 PIAS proteins and regulation of immune signaling

CREB-binding protein-interaction motifs (LXXLL) were first described in nuclear receptor (NR) proteins as being important for the interaction between receptor-ligand complexes and transcriptional coactivators such as p300 and CBP [44]. These motifs have since been implicated in both activating and disrupting signaling cascades through their ability to bind transcription factors, co-activators, and co-repressors [45, 46]. In particular, members of the mammalian Protein Inhibitor of Activated Stat (PIAS) family rely upon LXXLL motifs to inhibit JAK-STAT signaling in myriad ways. The PIAS family consists of PIAS1, PIAS3, PIASx (also called PIAS2), and PIASy (also called PIAS4), four factors with significant sequence identity, including the N-terminal SAP domain that contains a signature LXXLL motif [47].

The first evidence for the involvement of PIAS proteins in STAT regulation showed that PIAS3 specifically inhibited Stat3 by binding to it and blocking its DNA-binding activity [48].

Since then, PIAS1 has also been shown to inhibit DNA binding of STAT1 and NF-κB p65 [49]. PIAS proteins can also inhibit transcription by recruiting co-regulators, such as histone deacetylases, as in the cases of PIASx isoform β inhibiting STAT4-dependent gene activation and PIASy repressing activity of SMAD3 [47]. Third, PIAS proteins are capable of repressing transcription by sumoylating transcription factors, as in the case of PIAS1 or PIAS3 and STAT1 [50]. While the LXXLL motifs of these PIAS proteins were not always shown to be necessary for interaction between a PIAS and its target STAT, they were shown to be necessary for the repression of a given STAT by PIAS [47, 51, 52]. Finally, PIAS proteins are also capable of sequestering transcription factors such as LRIF1 in nuclear or sub-nuclear structures [47]. Thus, LXXLL-containing PIAS proteins have been shown to interfere with STAT and NF-κB immune signaling pathways, among others.

Chapters 2 and 3 of this work explore the role of human DUX4 and mouse Dux, two (L)LXXL(L)-containing proteins, on immune signaling in response to double-stranded RNA, double-stranded DNA, and Type-I and Type-II interferons. This work represents the first mechanistic study of the modulation of immune signaling by DUXC-family proteins and has important implications both for understanding FSHD disease activity and how immune-privileged tissues are established and maintained in early development.

1.4 CIC-DUX4 rearrangements

Previously, our lab and others have described a role for full-length DUX4 protein in cancers. However, there are also multiple types of cancer containing genetic rearrangements between *DUX4* and other genetic loci.

The majority of EWSR1 fusion-negative small blue round cell sarcomas harbor a genetic rearrangement of the transcription repressor CIC and DUX4 that results in a oncoprotein containing the N-terminal portion of CIC (containing its DNA-binding HMG box) fused to the C-terminal (L)LXXL(L)-containing activation domain of DUX4 [24, 53]. This fusion results in enhanced transcriptional activity of CIC, and the CIC-DUX4 oncoprotein upregulates the PEA3 subfamily of ETS transcription factors as in other Ewings-family tumors. However, a large-cohort study of CIC-rearranged sarcomas showed significantly lower 5-year survival rates when compared to patients with classical Ewings sarcomas [54], and these tumors are now thought to be a distinct and aggressive tumor subtype [55, 56]. Recently, a novel human CIC-DUX4 sarcoma cell line was established that will allow for testing of new therapeutic regimens *in vitro* [57].

A separate subtype of DUX4-rearrangement cancers includes B-cell acute lymphoblastic leukemia (B-ALL), which are characterized by genetic fusion between the *DUX4* locus and either the *IGH* or *ERG* loci. These independent genetic rearrangements appear to be the result of the insertion of a partial *DUX4* gene into the novel locus, though neither result in fusion protein expression [58]. Instead, the insertion of the *DUX4* gene at these loci allows it to piggyback on the regulatory regions of the partner gene, leading to DUX4 expression [58, 59]. As most of these *DUX4* insertions only contain partial genes, few led to expression of full-length DUX4 protein; instead, most resulting DUX4 proteins are truncated between aa312 to aa420 of the total 424aa, losing all or most of the C-terminal activation domain but consistently retaining the N-terminal DNA-binding homeodomains [58, 60].

Chapter 2 of this work establishes that the CIC-DUX4 fusion protein is capable of suppressing the transcriptional response to Type-II IFNγ. This has fascinating implications for

the efficacy of immunotherapies in treating CIC-DUX4 sarcomas and could provide insight as to how and why these tumors are so aggressive and go unchecked by the immune system.

Chapter 2: Human DUX4 and mouse Dux interact with STAT1 and broadly inhibit interferon-stimulated gene induction.

A version of this chapter is currently in review at *eLife* as:

Human DUX4 and mouse Dux interact with STAT1 and broadly inhibit interferon-stimulated gene induction.

Amy E Spens, Nicholas A Sutliff, Sean R. Bennett, Amy E. Campbell, and Stephen J. Tapscott.

2.1 Introduction

Double homeobox (DUX) genes encode a family of transcription factors that originated in placental mammals, consisting of DUXA, DUXB and DUXC subfamilies that all have similar paired homeodomains. The DUXC family is characterized by a small conserved region at the carboxy-terminus of the protein that includes two (L)LxxL(L) motifs and surrounding conserved amino acids [28]. Members of this family, including mouse *Dux* and human *DUX4*, are expressed in a brief burst at early stages of development and regulate an initial wave of zygotic gene activation [25-27]. While *DUX4* expression has also been reported in testes and thymus [61, 62], it is silenced in most somatic tissues.

Mis-expression of *DUX4* in skeletal muscle is the cause of facioscapulohumeral muscular dystrophy (FSHD) [30, 63], the third most prevalent human muscular dystrophy. DUX4 expression in skeletal muscle activates the early embryonic totipotent program, suppresses the skeletal muscle program, and ultimately results in muscle cell loss. Many of the genes induced by DUX4 in skeletal muscle encode proteins that are normally restricted to immune-privileged tissues [22] and their expression in skeletal muscle could induce an immune response. In this context it is interesting that FSHD muscle pathology is characterized by focal immune cell infiltrates. However, our prior studies have also suggested that DUX4 might suppress antigen presentation and aspects of an immune response. Expression of DUX4 in cultured muscle cells blocked lenti-viral induction of innate immune response genes such as *IFIH1* [22]. More recently we reported that expression of DUX4 in primary cancers and engineered cancer cell lines blocks the interferon-gamma (γ) mediated induction of MHC Class I antigen presentation and promotes resistance to immune checkpoint blockade treatments, such as anti-CTLA-4 and anti-PD-1

therapies [64]. The scope and mechanism(s) of how DUX4 suppresses immune signaling remains unknown.

DUX4 contains one LxxLL and one LLxxL motif at its C-terminal end that are among the most highly conserved regions of DUXC-family [28]. LxxLL motifs are alpha-helical protein-interaction domains that were first identified in nuclear-receptor signaling pathways [44]. Proteins containing LxxLL motifs, such as the Protein Inhibitor of Activated STAT or PIAS family, have been shown to modulate immune signaling of STATs, IRFs, NF-kB, and other transcription factors [47]. PIAS proteins block the function of these transcription factors in four ways: preventing DNA binding, recruiting co-repressors, stimulating SUMOylation, or sequestering them within nuclear or sub-nuclear structures [47].

In this study we show that a transcriptionally inactive C-terminal fragment of DUX4 is sufficient to block IFNγ-induction of most interferon stimulated genes (ISGs) and this requires the (L)LxxL(L) domains. Immunoprecipitation and mass spectrometry identified the IFNγ-signaling effector STAT1 and several other proteins involved in immune signaling as proteins that interact with the DUX4 C-terminal domain (DUX4-CTD). We show that the DUX4-CTD interacts with STAT1 phosphorylated at Y701 and interferes with stable DNA binding, recruitment of Pol-II, and transcriptional activation of interferon stimulated genes (ISGs). Consistent with these mechanistic studies, endogenous DUX4 in FSHD muscle cells and the CIC-DUX4 fusion protein expressed in a subset of EWSR1-negative small blue round cell sarcomas suppress IFNγ-induction of ISGs. The comparable CTD of mouse Dux containing (L)LxxL(L) motifs similarly interacts with STAT1 and blocks IFNγ stimulation of ISGs. These findings suggest an evolved role of the DUXC family in modulating immune signaling pathways and have implications for the role of DUX4 in development, cancers, and FSHD.

2.2 Results

2.2.1 DUX4 broadly suppresses interferon-stimulated gene (ISG) induction

Our prior studies showed that DUX4 inhibited ISG induction in response to lentiviral infection and suppressed induction of MHC Class I proteins in response to interferon-gamma (IFNγ, Type-II interferon) [22, 64]. To determine whether DUX4 broadly inhibited ISG induction by IFNγ we used the MB135-iDUX4 cell line, a human skeletal muscle cell line with an integrated doxycycline inducible DUX4 (iDUX4) transgene [65]. (See **Fig 8** for schematics and sequences of the transgenes used in this study.) Doxycycline induction of DUX4 expression in the MB135-iDUX4 cell line has been validated as an accurate cell model of the transcriptional consequences of DUX4 expression in FSHD muscle cells [65] and in the early embryo [25, 26]. Using a stringent 8-fold induction cut-off (log2 fold-change > 3), RNA-seq showed that IFNγ treatment induced 113 genes, whereas the expression of DUX4 suppressed ISG induction by IFNγ more than 4-fold for 76 (67%) of these genes and more than 2-fold for 102 genes (90%) (**Table 1**).

Informed by the RNA-seq results, we used RT-qPCR to measure the response of four ISGs that represent different components of the response to immune signaling: the RNA helicase *IFIH1*; the interferon-stimulated exonuclease *ISG20*; the chemoattractant *CXCL9*; and the major histocompatibility complex class II (MHC-II) chaperone *CD74*. IFNγ-induction of all four genes was robustly blocked by DUX4 expression while a DUX4-target gene *ZSCAN4* was strongly induced, indicating that the ISG suppression did not represent a universal block to gene induction (**Fig 1**, MB135-iDUX4 and **Fig 9A (**for this and subsequent constructs, **Fig 9** shows RT-qPCR data from additional independent cell lines together with protein expression and nuclear localization)); whereas doxycycline treatment in the absence of iDUX4 did not suppress ISG

induction (**Fig 1**, MB135 parental). In contrast to DUX4, a paralog in the DUX family, DUXB, did not suppress ISG induction by IFNγ (**Fig 1**, MB135-iDUXB).

2.2.2 DUX4 transcriptional activity is not necessary for ISG suppression

There are two conserved regions of the DUX4 protein, the N-terminal homeodomains (aa19-78, aa94-153) and an ~50 amino acid region at the end of the C-terminal domain (CTD) that is required for transcriptional activation by DUX4 (aa371-424) [23, 28, 66]. A mutation in the first homeodomain, F67A, prevents DUX4 DNA binding and target gene activation [67]. When expressed in MB135 cells, iDUX4-F67A did not activate the DUX4 target gene *ZSCAN4* yet still suppressed ISG induction by IFNγ (**Fig 2A and B**, and **Fig 9B**). A second construct, iDUX4aa154-424, which has the N-terminal homeodomain region replaced by a 3x FLAG tag and nuclear localization signals (3xFLAG-NLS) cassette (hereafter called iDUX4-CTD), was also transcriptionally silent yet equally suppressed activation of ISGs (**Fig 2A and C** and **Fig 9C**). RNA sequencing analysis using the same criteria to characterize ISG suppression by the full-length DUX4 demonstrated that the F67A mutant suppressed 70% of induced genes by more than 2-fold, or 41% of induced genes by more than 4-fold; whereas the iDUX4-CTD showed 90% or 52% suppression, respectively (**Table 1**). Together, these data indicate that DUX4 transcriptional activity is not necessary to suppress IFNγ-mediated gene induction.

2.2.3 The C-terminal Domain (CTD) is necessary and sufficient to suppress ISGs

The DUX4-CTD contains a pair of (L)LxxL(L) motifs, LLDELL and LLEEL, that are conserved across the DUXC/DUX4 family [28]. DUX4 transgenes with mutations in the first motif, deletion of the second motif, or both (iDUX4mL1, iDUX4dL2, iDUX4mL1dL2) (see **Fig**

9 for sequences of these mutants) failed to activate the DUX4 target *ZSCAN4* (**Fig 2A**). iDUX4ml1dl2 and iDUX4dl2 both lost the ability to suppress the panel of ISGs, whereas iDUX4mL1 showed partial activity, suppressing 3 of the 4 ISGs (**Fig 2D and Fig 9D**), indicating that these (L)LxxL(L) motifs are necessary for both ISG suppression and for transcriptional activation by DUX4.

To test sufficiency, we generated two additional C-terminal fragments of DUX4 (**Fig 2C**). The first, iDUX4-CTDmL1dL2, contains the CTD of iDUX4mL1dL2 with its N-terminal HDs replaced with the 3xFLAG-NLS cassette. Similar to iDUX4mL1dL2, iDUX4-CTDmL1dL2 did not block the panel of ISGs (**Fig 2C and Fig 9E)**. The second construct, iDUX4aa339-424, contains only the C-terminal 85 aa residues including both (L)LxxL(L) motifs, and maintained ISG suppression, though not as strongly on the *IFIH1* and *ISG20* genes (**Fig 2C and Fig 9F**). In summary, these data support a model in which the DUX4-CTD is both necessary and sufficient to suppress a major portion of the ISG response to IFNγ.

2.2.4 The DUX4 protein interacts with STAT1 and additional immune response regulators

As an unbiased method to identify proteins that interact with the C-terminal region of DUX4, we used liquid chromatography mass spectroscopy (LC-MS) to identify proteins that co-immunoprecipitated with DUX4-CTD constructs expressed in MB135 myoblasts. In the first experiment, we used MB135iDUX4-CTD cells either untreated, treated with doxycycline alone, or with both doxycycline and IFNγ. In the second experiment, we used MB135iDUX4-CTD and MB135iDUX4mL1dL2 cells both treated with doxycycline and IFNγ, compared to these two cell lines untreated and combined as a control. Proteins with a minimum of 2 peptide spectrum matches (PSMs) in at least one sample that were identified in both experiments were assigned to

one of ten categories (see Methods) to separate candidate interactors from other categories that might be co-purified because of obligate interactions (e.g., proteasome or ribosome) or might be less likely to be relevant to immune responses (e.g., cytoskeletal proteins). Candidate interactors were then ranked based on the total PSMs for that protein across all samples. (It is important to note that the "bait" constructs were expressed at low levels in the samples not treated with doxycycline and that the immunoprecipitation concentrated this background, which might account for some of the candidate proteins appearing in the untreated samples.) STAT1 and DDX3X, two key regulators of innate immune signaling, ranked at the top of the list of candidate DUX4-CTD interactors, together with several other proteins implicated in modulating innate immune signaling (**Fig 3, left table**). Western blot analysis using independent biological samples from a co-IP experiment with MB135-iDUX4-CTD and MB135-iDUXB (as a control) validated the DUX4-CTD interactions with DDX3X, STAT1, PRKDC, YBX1, HNRNPM, PABPC1, NCL, CDK4, and HNRPU (**Fig 3, right panel**).

2.2.5 The DUX4-CTD preferentially interacts with STAT1 phosphorylated at Y701

Because of its central role in IFNγ signaling, we elected to focus on the interaction of STAT1 with DUX4. To map the region(s) of the DUX4-CTD necessary to interact with STAT1, we expressed a truncation series in MB135 cells (all with an N-terminal 3xFLAG tag and NLS and all treated with IFNγ): iDUX4-CTD (aa154-424), iDUX4aa154-372, iDUX4aa154-308, and iDUX4aa154-271. The region of DUX4 between amino acids 271 and 372 was necessary for co-IP of STAT1, whereas the region between 372 and 424 containing the (L)LxxL(L) motifs might enhance DUX4-CTD binding to the phosphorylated forms of STAT1 (**Fig 4A**).

To determine whether phosphorylation of STAT1 enhanced interaction with DUX4, we co-expressed the FLAG-tagged iDUX4-CTD with a MYC-tagged iSTAT1 or STAT1 mutants Y701A or S727A, wherein doxycycline would induce expression of both the DUX4 and STAT1 transgenes. The wild-type STAT1 and STAT1-S727A showed enhanced binding to the CTD with IFNγ treatment, whereas IFNγ did not enhance the binding of STAT1-Y701A (**Fig 4B**). Furthermore, the interaction of *in vitro* translated iDUX4-CTD with *in vitro* translated STAT1, but not STAT1 Y701A, was enhanced by treatment with the JAK1 kinase to phosphorylate Y701 (**Fig 4C**). Finally, immunofluorescence showed that DUX4-CTD expression did not prevent translocation of STAT1 to the nucleus following IFNγ treatment (**Fig 10**) and proximity Ligation Assay (PLA) indicated close interaction between the iDUX4-CTD and endogenous pSTAT1-Y701 in the nucleus of MB135 cells treated with doxycycline and IFNγ (**Fig 4D**). Therefore, the interaction between DUX4-CTD and STAT1 is enhanced by phosphorylation of STAT1-Y701 and this interaction happens within the nuclei of DUX4-CTD expressing cells.

2.2.6 The DUX4-CTD decreases STAT1 occupancy at ISG promoters and blocks Pol-II recruitment

Chromatin immunoprecipitation (ChIP) was performed on MB135-iDUX4-CTD cells to assess STAT1 binding to ISG promoters. Compared to a gene-desert region where there should not be STAT1 binding (h16q21), there was a robust induction of STAT1 binding following IFNγ treatment at the promoters of several ISGs (*GBP1*, *IDO1*, *CXCL10*) with previously characterized STAT1 binding sites [68] (**Fig 5A, left four panels**). Treatment with IFNγ following induction of DUX4-CTD diminished STAT1 occupancy at all three ISGs, and paired RT-qPCR confirmed that the DUX4-CTD robustly suppressed the RNA induction by IFNγ (**Fig**

5A, right panel). We used CUT&Tag (Cleavage Under Target & Tagmentation) [69] to assess Pol-II occupancy genome wide and found that DUX4-CTD blocked Pol-II recruitment to ISGs without affecting occupancy at other genes (**Fig 5B**).

2.2.7 Endogenous DUX4 expression in FSHD myotubes is associated with suppressed ISGs

Although DUX4 is expressed at very low levels in cultured FSHD muscle cells, the low levels in the population reflects high expression in a small population of cells [61, 70]. For example, in cultured FSHD myotubes, approximately 5% of the myotubes might express DUX4 in their nuclei. To determine whether endogenous DUX4 suppresses IFNγ signaling, we assessed IFNγ induction of IDO1 in FSHD myotubes. Differentiation of FSHD myoblasts into multinucleated myotubes results in distinct populations of DUX4-expressing and DUX4-negative myotubes in the same culture, allowing for side-by-side evaluation of DUX4-positive and DUX4-negative muscle cells in the same culture. We determined the IFNγ induction of IDO1 as a representative ISG based on its low basal expression in skeletal muscle and our prior demonstration that it is suppressed in the MB135-iDUX4-CTD cells (see **Fig 5B, right panel**). Treatment with IFNγ produced a reliable IDO1 signal within the nucleus and cytoplasm of individual myotubes that did not express DUX4, whereas DUX4-positive myotubes did not show IDO1 expression in response to IFNγ (**Fig 6A**). Therefore, similar to our MB135-iDUX4 studies, endogenous DUX4 expressed at a physiological level is sufficient to prevent ISG induction by IFNγ.

2.2.8 Endogenous CIC-DUX4 fusion gene suppresses ISG induction in a sarcoma cell line

The majority of EWSR1 fusion-negative small blue round cell sarcomas have a genetic re-arrangement between CIC and DUX4 that creates a fusion protein containing the carboxyterminal (L)LxxL(L) motif region of DUX4 [24, 53]. We confirmed that the Kitra-SRS sarcoma cell line expresses a CIC-DUX4 fusion mRNA containing the terminal 98 amino acids of DUX4 as previously described [57]. Compared to MB135 myoblasts, Kitra-SRS cells showed absent-to-low induction of ISGs when treated with IFNγ and control siRNAs. In contrast, siRNA knockdown of the CIC-DUX4 fusion in the Kitra-SRS cells resulted in a substantially increased IFNγ-induction of ISGs, whereas knockdown of CIC in the MB135 cells did not alter ISG induction **(Fig 6B).**

To confirm that the CIC-DUX4 fusion was suppressing ISG induction, we expressed a doxycycline inducible CIC or the Kitra-SRS CIC-DUX4 fusion protein in MB135 cells and showed that the CIC-DUX4 fusion, but not CIC, suppressed IFNγ-induction of ISGs *IFIH1*, *CXCL9*, and *CD74*, although not *ISG20* (**Fig 6C**).

2.2.9 Conservation of ISG repression and STAT1 interaction in mouse Dux

Dux, the mouse ortholog of human *DUX4*, is expressed at the equivalent developmental stage to human *DUX4* [25], activates a parallel transcriptional program [26], and contains the (L)LxxL(L) motifs that we have shown to be necessary for ISG repression by human DUX4. In fact, the mouse Dux sequence contains a 60 amino acid triplication of the (L)LxxL(L)-containing region (**Fig 11**). Accordingly, we introduced a doxycycline-inducible mouse *Dux* transgene into human MB135 cells (MB135-iDux) and found that the full-length Dux protein repressed the panel of ISGs even more robustly than the full-length or CTD portion of human DUX4 (**Fig 7A**).

Similar to human DUX4, Western analysis confirmed the co-immunoprecipitation of STAT1 and both phosphorylated pSTAT1-Y701 and pSTAT1-S727 with mouse Dux (**Fig 7A**). These data demonstrate that the suppression of ISG induction and interaction with phosphorylated STAT1 is conserved in the DUXC family.

2.3 Discussion

In this chapter, I showed that the DUX4-CTD, a transcriptionally inactive carboxyterminal fragment of DUX4, is necessary and sufficient to broadly suppress ISG induction by IFNγ. The DUX4-CTD colocalizes with STAT1 in the nucleus, diminishes STAT1 occupancy at ISG promoters, and prevents Pol-II recruitment and transcriptional activation of ISGs by IFNγ. Whereas the conserved DUX4 (L)LxxL(L) motifs are necessary to suppress transcriptional activation by STAT1, they are not necessary for the interaction of DUX4 and STAT1. The suppression of IFNγ signaling by endogenous DUX4 in FSHD muscle cells and the CIC-DUX4 fusion protein in sarcomas provides support for the biological relevance of these findings.

My data support a simple model of how DUX4 inhibits STAT1 activity (**Fig 7B**). Under normal circumstances, IFNγ binding to its receptor, IFNGR, leads to the phosphorylation of STAT1 at Y701. Subsequently, STAT1 forms a homodimer, translocates to the nucleus, and binds the gamma-activated sequence (GAS) in the promoters of ISGs. DNA-bound STAT1 is additionally phosphorylated at S727 and recruits Pol-II to the ISG promoters [71, 72]. Our studies show that the DUX4-CTD interacts with STAT1 phospho-Y701 in the absence of phospho-S727 (i.e., binds the S727A STAT1 mutant), yet also efficiently co-immunoprecipates with STAT1 phospho-S727 from cell lysates. This indicates that despite DUX4 binding to

STAT1 phospho-Y701, DNA binding of this complex is not fully impaired because of the association with STAT1 phospho-727. However, our ChIP and CUT&Tag studies show decreased STAT1 steady-state occupancy of ISG promoters and failure to recruit Pol-II. Together, these data support a model of DUX4 interaction with pSTAT1-Y701 that prevents the formation of a stable DNA bound complex and recruitment of Pol-II, but likely not the initial binding of STAT1 to DNA because of the abundance of phospho-S727 associated with DUX4. The (L)LxxL(L) motifs are necessary to prevent transcriptional activation, presumably by blocking Pol-II recruitment, but not necessary for the interaction of DUX4 with STAT1. This could be due to recruitment of a repressor, or by simply blocking the interaction of STAT1 with an intermediate factor necessary to recruit Pol-II.

The (L)LxxL(L)-dependent inhibition of STAT1 by DUX4 in the current study bears a striking similarity to the inhibitory mechanisms displayed by LxxLL-containing members of the PIAS family. LxxLL motifs were first identified in nuclear-receptor (NR) signaling pathways [44] where they were found to facilitate protein-protein interactions between unbound NRs and co-repressors such as RIP140 and HDACs, or agonist-bound NRs and co-activators such as CBP/p300 [45, 73]. LxxLL motifs have since been characterized in multiple protein families, including the PIAS family, and specifically implicated in modulating immune transcriptional networks via interaction with and inhibition of STATs, IRFs, and NF-kB [47]. While the (L)LxxL(L) region of DUX4 is required for suppression of IFNγ-mediated ISG induction and its enhanced interaction with pSTAT1-Y701, it is not required for its apparently weaker interaction with unphosphorylated STAT1. In a similar manner, the LxxLL motif of PIASγ is not required for initial binding to STAT1, but is required to suppress ISG induction mediated by STAT1 in response to both IFNβ [74] and IFNγ [51]. The same motif is required for the trans-repression of

androgen receptor (AR) signaling by PIASγ [75] and of Erythroid Krüppel-like factor (EKLF or KLF1) by PIAS3 [76], though again it is not required for the initial interaction of either pair. The studies referenced above hypothesize that this trans-repression relies on the recruitment of co-repressors, although the specific interactors were not determined. Additionally, just as DUX4 reduces the steady-state occupancy of STAT1 to DNA, PIAS proteins can suppress transcriptional networks by blocking DNA binding, as with PIAS3 and STAT3 [48] or PIAS1 and NF-kB p65 [52]. These studies describe mechanisms of transcriptional suppression by LxxLL motifs in PIAS and other proteins that have strong parallels to the (L)LxxL(L) motifs in human DUX4 and mouse Dux. It is important to emphasize that the xx amino acids in the DUXC family are acidic and there is conservation of flanking amino acids as well, suggesting that the DUXC family likely evolved target specificity through these larger areas of conservation.

In addition to STAT1, the mass spectrometry identified several proteins that interact with the DUX4-CTD that might also have a role in modulating immune signaling. Although additional work is needed to validate the biological relevance of these interactions, many have functions related to immune signaling and that will need to be evaluated in future studies. DDX3X and PRKDC are the top ranked candidates, together with STAT1. DDX3X has been shown to regulate RNA processing, translation, and innate immune signaling [77]. It was also shown to be a pathway specific regulator of IRF3 and IRF7 in part by acting as a scaffolding factor necessary for IKK-ε and TBK1 phosphorylation of IRFs [78, 79]. DDX3X was also shown to be a sensor of dsRNA and viral stem-loop RNA with a role in the initial induction of ISGs, including IFIH1 and DDX58 [80] that then serve to amplify the signaling mechanisms. PRKDC is known mostly for its major roles in DNA repair but also has been implicated in regulating the response to cytoplasmic DNA through the cGAS and IRF3 pathway [81].

Our current findings also provide a molecular mechanism for the suppression of IFNγ stimulated genes in DUX4-expressing cancers. Previously we reported that the full-length DUX4 is expressed in a diverse set of solid cancers [64]. Cancers expressing DUX4 had diminished IFNγ-induced MHC Class I expression, reduced anti-tumor immune cell infiltration, and showed resistance to immune checkpoint blockade. In our current study, we show that the CIC-DUX4 fusion in EWSR1-fusion-negative sarcomas blocks IFNγ-induced ISG expression. This fusion protein contains the terminal 98 amino acids of DUX4, aa327-424, that encompasses a region shown to be sufficient to suppress IFNγ signaling in the iDUX4-aa339-424 (see **Fig 2C**). It is reasonable to suggest that this fusion protein in the CIC-DUX4 sarcomas, or the full length DUX4 in some other cancers, contributes to immune evasion, at least in part, through its interaction with STAT1, and that targeting DUX4 or its interaction with STAT1 might improve immune-based therapies for DUX4-expressing cancers.

The conservation of the (L)LxxL(L) motifs in mouse Dux and its similar interaction with STAT1 and inhibition of IFNγ signaling indicates that this is a conserved function of the DUXC family. DUX4, Dux, and the canine DUXC all induce expression of endogenous retroelements, as well as pericentromeric satellite repeats that form dsRNAs that, at least in the case of DUX4, induce a dsRNA response that results in activation of PKR and phosphorylation of EIF2α [82, 83]. Therefore, it is possible that the interaction with STAT1 and other immune signaling modulators might prevent the activation of the ISG pathway while permitting the PKR response, although the biological consequences remain to be further explored. It is also interesting that DUX4, Dux and possibly other members of the DUXC family are expressed in immune privileged tissues—i.e., cleavage embryo, testis, and thymus—and our study suggests that their expression might contribute to this immune privileged state.

2.4 Materials and Methods

Cell culture

All experiments were conducted in immortalized MB135 or MB200 myoblast cell lines (isolated from a control or FSHD2 subject, respectively cultured in Ham's F-10 Nutrient Mix (Gibco) supplemented with 15% fetal bovine serum (Hyclone), 100 U/100 µg/ml penicillin/streptomycin (Gibco), 1µM dexamethasone (Sigma), and 10ng/mL recombinant human basic fibroblast growth factor (PeproTech). To differentiate the myoblasts to myotubes, media was changed to DMEM supplemented with 10 ug/ml insulin (Sigma) and 10 ug/ml transferrin (Sigma). Cell lines containing doxycycline-inducible transgenes were additionally cultured with 2 µg/mL puromycin (Sigma). Transgenes were induced with 1 µg/mL of doxycycline (Sigma) for 4 hours prior to other treatments for a total of 20 hrs.

Cloning, virus production, and monoclonal cell line isolation

Human DUX4 and mouse Dux truncation constructs were created by cloning synthesized, codon-optimized gBlock fragments into the pCW57.1 vector (Addgene plasmid #41393) downstream of the doxycycline-inducible promoter. Lentiviral particles were created by transfecting 293T cells with the subcloned pCW57.1 expression vectors, psPAX2 (Addgene plasmid #12260), and pMD2.G (Addgene plasmid #12259) using Lipofectamine 2000 according to the manufacturer's instructions (Invitrogen). Myoblasts were transduced and selected using 2 µg/mL puromycin at low enough confluence to allow for isolation of clonal lines using cloning cylinders. Transgenic clonal lines were validated for protein size, expression level, and localization by western blot and immunofluorescence.

Immune stimulation and RT-qPCR

Myoblasts were transfected with (final concentration) 200 ng/mL IFNγ (R+D Systems) by addition directly to cell culture medium. After 16 hours of immune stimulation, RNA was collected from cells using the NucleoSpin RNA Kit (Macherey-Nagel) according to manufacturer's instructions. RNA samples were quantified by nanodrop and 1 μg of RNA per sample was treated with DNase I Amplification Grade (Thermo Fisher), and then synthesized into cDNA using the Superscript IV First-Strand Synthesis System, including oligo dT primers (Invitrogen). qPCR was run in 384-well plates on an Applied Biosystems QuantStudio 6 Flex Real-Time PCR System (ABI) and analyzed in Microsoft Excel.

RNA-seq Library Preparation and Sequencing

RNA was extracted as described above from untreated, doxycycline-treated, IFNγ-treated, or doxycycline- and IFNγ-treated samples. RNA was submitted to the Fred Hutchinson Cancer Research Center Genomics Core for library preparation using the TruSeq3 Stranded mRNA kit (Illumina) followed by size and quality analysis by Tapestation (Agilent). Libraries were sequenced on a NextSeq P2-100 (Illumina).

Immunofluorescence

Cells were fixed for 10 minutes with 2% paraformaldehyde (Thermo Scientific) for DUX4/STAT1 and 4% paraformaldehyde for DUX4/IDO1 then permeabilized for 10 minutes with 0.5% Triton X-100 (Sigma), both at room temperature with gentle shaking. Cells were then blocked for 2 hours with PBS/0.3M glycine/3% BSA at room temperature with gentle shaking. Primary antibodies were incubated at 4^{o}C overnight: mouse anti-FLAG M2 1:500 (Sigma

#F1804), rabbit anti-STAT1 mAb 1:750 (Abcam #ab109320), rabbit anti-IDO1 (D5J4E) 1:100 (Cell Signaling Tech 86630S), and mouse anti-DUX4 (P2G4) 1:250 [66]. Cells were washed three times with 1X PBS containing 3% BSA, then secondary antibodies were incubated for 1hr at room temperature: FITC-conjugated donkey anti-rabbit (Jackson ImmunoResearch) or TRITC-conjugated donkey anti-mouse (Jackson ImmunoResearch). Cells were washed once with 1X PBS containing 3% BSA then stained with DAPI (Sigma) for 10' at room temperature and then visualized.

Fractionated anti-FLAG immunoprecipitation

Cells were lysed on the plate with digitonin lysis buffer pH 7.4 (37.5 μg/mL digitonin, 25 mM Tris-HCl pH 7.5, 125 mM NaCl, 1 mM EDTA, 5% glycerol) supplemented with Pierce Protease Inhibitors EDTA-free (PIA32955) and Pierce Phosphatase Inhibitors (PIA32957), transferred to a centrifuge tube and incubated for 10 minutes at 4°C with rotation. Centrifugation at 2500 rcf at 4ºC for 5 min pelleted the nuclei, supernatant was discarded, and nuclei resuspended in 1mL IP buffer pH 7.4 (25 mM Tris-HCl pH 7.5, 175 mM NaCl, 1 mM EDTA, 0.2% NP-40, 5% glycerol) and incubated for 1 hour at 4°C with rotation then spun at 21000 rcf for 10 minutes at 4ºC to pellet insoluble debris. Protein concentration was determined using the Pierce BCA Protein Assay Kit (ThermoFisher, 23225). An equivalent amount of protein per sample was pre-cleared with Dynabeads Protein G (Invitrogen) bound to mouse IgG (Abcam #131368) for 1 hour at 4°C with rotation. FLAG-tagged constructs were then immunoprecipitated with Dynabeads Protein G beads coupled to mouse anti-FLAG M2 mAb (Sigma F3165) for 3 hours at 4°C with rotation. Beads were washed 3X with 1 mL IP buffer and

eluted by adding 2X NuPage LDS Sample Buffer (Thermo Fisher, diluted from 4X with PBS) to the beads and heating for 10 minutes at 70°C.

Liquid Chromatography Mass Spectroscopy (LC-MS)

For LC-MS, anti-FLAG immunoprecipitation was performed with beads cross-linked to the anti-FLAG antibody and the proteins competitively eluted with FLAG peptide. Eluted protein samples were electrophoresed into a NuPage 4-12% Bis-Tris gel, excised, and processed by the Fred Hutchinson Cancer Research Center Proteomics Core. Samples were reduced, alkylated, digested with trypsin, desalted, and run on the Orbitrap Eclipse Tribid Mass Spectrometer (Thermo Fisher). Proteomics data were analyzed using Proteome Discoverer 2.4 against a Uniprot human database that included common contaminants using Sequest HT and Percolator for scoring. Results were filtered to only include protein identifications from high confidence peptides with a 1% false discovery rate. Proteins that were identified in at least one sample from both independent experiments with at least 2 PSMs in one sample were assigned to one of ten categories: 1, candidates; 2, cytoskeletal associated; 3, cytoskeletal; 4, ribosome/translation associated; 5, proteasome associated; 6, membrane or extracellular; ER, golgi, or vesicle associated; 8, lipid metabolism; 9, chaperones; 10, nuclear import or nuclear membrane associated. The proteins in category 1 were further investigated for interactions with DUX4. It should be noted that this category assignment process de-prioritized groups of proteins based on assignment to a cellular compartment or function (e.g. ribosome/translation proteins might associate with DUX4 as part of a translation complex rather than having a role in immune signaling) and it is possible that some of the proteins assigned to the non-candidate categories might be functional interactors with DUX4 and have an important biological role.

Chromatin immunoprecipitation and sequencing

Chromatin immunoprecipitation (ChIP) was performed as previously described (Nelson *et al* 2006) with the following modifications: Cells were plated and allowed to grow to 70-80% confluence. Pelleted nuclei were sonicated on a Diagenode Biruptor on "Low" for 10 min as 30 sec on/30 sec off, followed by 6 rounds of sonication on "High" for 10 min each as 30 sec on/30 sec off (70 minutes total sonication) in IP Buffer + 0.5% SDS. For immunoprecipitation, 500 ng of chromatin was set aside per condition as an "Input" and 4 µg of antibody was added to 10 µg of chromatin in an equal volume of IP Buffer + 0.5% SDS across samples. IP Buffer (150mM NaCl, 50mM Tris-HCl pH 7.4, 5mM EDTA, 1% Triton X-100, 0.5% NP-40, +Roche cOmplete mini protease inhibitor EDTA-free) was added to lower the percentage of SDS < 0.1%, and tubes were incubated with rotation overnight at 4°C. During this time, protein-A agarose Fastflow beads (Millipore) were washed twice with IP Buffer and then blocked in IP Buffer containing 2% BSA by rotating overnight at 4°C. After clearing the chromatin as described, beads were aliquoted to fresh tubes and the top 90% of chromatin was transferred to the tubes containing the blocked bead slurry. Tubes were rotated for 1 hour at 4°C. Beads were washed (definition of a "wash" in the protocol) 5 times with cold IP Buffer containing 0.1% SDS, 2 times with cold IP Buffer containing 500mM NaCl, and 2 times with cold PBS. DNA was isolated as described in the original protocol and used as a template in qPCR. Input DNA was used to create a standard curve. qPCR primers were previously published [68, 84] for ISGs and h16q21, respectively.

RNA-seq Analysis

Sequencing analysis was performed using R version 4.0.3 (R Core Team, 2020). Sequencing reads were trimmed using Trimmomatic (version 0.39) [85], and aligned to the

Homo sapiens GRCh38 reference genome with the Rsubread aligner [86]. Gene counts were analyzed using featureCounts (v2.0.1) [86] and the Gencode v35 annotation file. Normalization and differential expression analysis were done with DESeq2 (v1.26.0) [87].

In vitro transcription, translation, and immunoprecipitation

In vitro translated proteins were prepared using the TnT Quick Coupled Transcription Translation System (Promega, L2080) for the SP6 promoter on the pCS2 plasmids containing the construct of interest. Following translation, 1uL of each reaction was used for SDS-Page and western blotting to determine relative amounts of protein between constructs by quantification of band intensity. To phosphorylate the 3xMYC-STAT1 protein at Y701, *in vitro* translated protein was incubated for 1 hour at 30ºC with 1X Kinase Buffer A (ThermoFisher, Cat# PV3189), 1mM ATP (ThermoFisher, Cat# PV3227), and recombinant JAK1 kinase (ThermoFisher, Cat# PV4774) at a concentration of 10ug/ml. For immunoprecipitation, FLAG-tagged bait proteins were mixed at equal concentrations with MYC-tagged STAT1 proteins, and then volumes were adjusted to 500uL with ice-cold *in vitro* IP buffer [20mM Tris-HCl pH 7.5, 137mM NaCl, 1mM EDTA, 0.1% Tween20, 5% glycerol, adjusted pH to 7.4]. Proteins were rotated overnight at 4ºC to facilitate protein interaction. Samples were pre-cleared with 30uL of Dynabeads Protein G bound to mouse IgG_1 (ThermoFisher, Cat#PI31903) for 3 hours at 4ºC. Then FLAG-tagged proteins were immunoprecipitated overnight at 4ºC with 50uL of Dynabeads Protein G bound to anti-FLAG [M2] (F3165). Samples were washed 3 times with 1mL of ice-cold IP wash buffer [25 mM Tris-HCl pH 7.5, 175 mM NaCl, 1 mM EDTA, 0.2% NP-40, 5% glycerol, adjusted pH to 7.4], and then eluted with 30uL 2x NuPage LDS Sample Buffer (diluted with IP buffer) for 10 minutes at 70ºC and 1000rpm.

Proximity Ligation Assay

Cells were fixed for 10 minutes with 4% paraformaldehyde (Thermo Scientific), permeabilized for 10 minutes with 0.5% Triton X-100 (Sigma), and then blocked for 2 hours at room temperature with PBS/0.3M glycine/3% BSA. Primary antibodies were diluted in PBS/3% BSA and incubated with samples overnight at 4^{o}C: anti-FLAG [M2] (F1804) (1:4000), anti-STAT1 [EPR4407] (1:1000), and anti-pSTAT1 Y701 [58D6] (1:1000). Samples were washed 3 times for 10 minutes with 1x Wash Buffer A [10mM Tris, 150mM NaCl, 0.05% Tween, adjusted pH to 7.4], and then incubated with Duolink In Situ PLA Probe Anti-Rabbit PLUS (Sigma, Cat# DUO92002) and Duolink In Situ PLA Probe Anti-Mouse MINUS (Sigma, Cat# DUO92004) diluted in PBS/3% BSA for 1 hour in a humidity chamber at 37^{o}C. Samples were washed 3 times for 10 minutes with 1x Wash Buffer A, and then treated with ligase from the Duolink In Situ Detection Reagents Green kit (Sigma, Cat# DUO92014) for 30 minutes in a humidity chamber at 37^{o}C. Samples were washed 3 times for 10 minutes with 1x Wash Buffer A, and then treated with polymerase from the Duolink In Situ Detection Reagents Green kit for 1 hour and 40 minutes in a humidity chamber at 37^{o}C. Samples were washed 2 times for 10 minutes with 1x Wash Buffer B [200mM Tris, 100mM NaCl, adjusted pH to 7.5] and then once for 1 minute with 0.01x Wash Buffer B. Samples were mounted with Prolong Glass Antifade Mountant (ThermoFisher, Cat# P36983), and then visualized with a fluorescent microscope using FITC and DAPI filters.

CUT&Tag

CUT&Tag was performed as previously described [69] with the following modifications: MB135-iDUX4-CTD myoblasts were plated and allowed to grow to 70-80% confluence. Cells

were left untreated, treated with 200ng/mL IFNγ for 16hr, or pre-treated with 1μg/mL doxycycline for 4hr then had IFNγ added directly to cell media for an additional 16hr. Fresh cells were harvested and washed in PBS, crosslinked with 0.1% formaldehyde for 90 seconds, then counted and 1.25e6 cells were aliquoted per reaction tube. *Drosophila* S2 cells were spiked-in at a genomic ratio of 1:10. Nuclei were prepared from cells in Buffer NE1 (20mM HEPES-KOH pH7.9, 10mM KCl, 0.1% Triton X-100, 20% glycerol, 0.5mM spermidine, 1x Roche cOmplete mini EDTA-free protease inhibitor) on ice for 10min and then bound to concanavalin A-coated beads for 10min. Primary antibody (dilution 1:50) was bound overnight at 4°C in 25μL per sample of Antibody Buffer (20mM HEPES-KOH pH7.5, 150mM NaCl, 0.5mM spermidine, 0.01% digitonin, 2mM EDTA, 1x Roche cOmplete mini EDTA-free protease inhibitor). Secondary antibody (dilution 1:100) was bound in 25μL per sample of Wash150 Buffer (20mM HEPES-KOH pH7.5, 150mM NaCl, 0.5mM spermidine, 1x Roche cOmplete mini EDTA-free protease inhibitor) for 30min at room temperature. pAG-Tn5 pre-loaded adapter complexes (Epicypher) were added to the nuclei-bound beads for 1hr at room temperature in 25μL of Wash300 Buffer (20mM HEPES-KOH pH7.5, 300mM NaCl, 0.5mM spermidine, 1x Roche cOmplete mini EDTA-free protease inhibitor), then beads were washed and resuspended in Tagmentation Buffer (Wash300 Buffer + 10mM $MgCl_2$) and incubated at 37°C for 1hr in a thermocycler with heated lid. Tagmentation was stopped by addition of EDTA, SDS, and proteinase K. DNA was extracted by Phenol-Chloroform and amplified by PCR using CUTANA High Fidelity 2x PCR Master Mix (EpiCypher) and cycling conditions: 5min at 58°C; 5min at 72°C; 45sec at 98°C; 14 cycles of 15sec at 98°C, 10sec at 60°C; 1min at 72°C. PCR products were cleaned up using SPRI beads (Agencourt) at a ratio of 1.3:1 according to manufacturer's instructions.

Antibodies

Antibodies against STAT1 [EPR4407] (ab109320), pSTAT1 Y701 [M135] (ab29045), pSTAT1 Y701 [58D6] (CST 9167), pSTAT1 S727 [EPR3146] (ab109461), YBX1 [EP2708Y] (ab76149), PABPC1 (ab21060), hnRNPM [EPR13509(B)] (ab177957), PRKDC [Y393] (ab32566), and HSP90AB1 [EPR16621] (ab203085) were purchased from Abcam. Antibodies against FLAG tag [M2] (F1804) and [M2] (F3146) were purchased from Sigma Aldrich. Antibodies against DDX3X [D19B4] (8192S), hnRNPK [R332] (4675S), TRIM28 [C42G12] (4124S), PPP2R1A [81G5] (2041S), NCL [D4C7O] (14574S), MYC tag [71D10] (2278S), IDO1 [D5J4E] (86630S), and Phospho-Rbp1 CTD (Ser5) [D9N5I] (13523S) were purchased from Cell Signaling Technology. Antibodies against hnRNPU (14599-1-AP), CDK4 (11026-1-AP), and HAT1 (11432-1-AP) were purchased from ProteinTech. The antibody against HSPA8 [SR39-04] (PIMA532002) was purchased from ThermoFisher. The antibody against DUX4 (P2G4) was described previously [66]. The antibodies Goat anti-Rabbit IgG HRP (ThermoFisher, A27036) and Rat anti-Mouse IgG HRP for IP (Abcam, ab131368) were used as secondary antibodies against rabbit and mouse primary antibodies for western blotting. The anti-Rabbit secondary antibody for CUT&Tag (13-0047) was purchased from Epicypher.

Figure 1. DUX4 suppresses interferon-stimulated gene (ISG) induction.

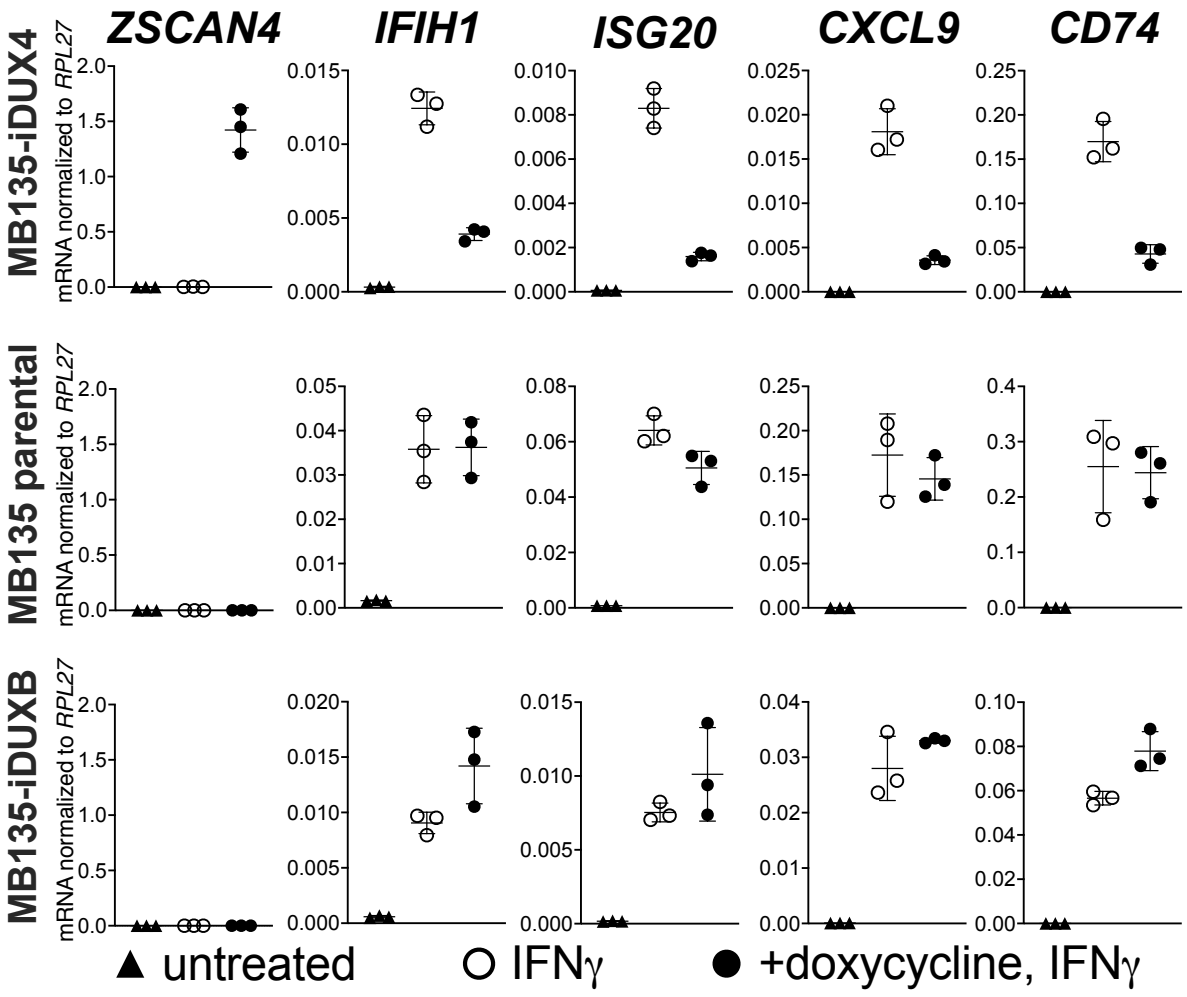

(**A**) MB135 cells expressing doxycycline-inducible DUX4 (MB135-iDUX4), parental MB135 cells, or MB135 cells expressing doxycycline-inducible DUXB (MB135-iDUXB) were untreated, treated with IFNγ, or treated with doxycycline and IFNγ. RT-qPCR was used to evaluate expression of a DUX4 target gene, *ZSCAN4*, and interferon-stimulated genes *IFIH1*, *ISG20*, *CXCL9*, and *CD74*. Ct values were normalized to the housekeeping gene *RPL27*. Data represent the mean ±SD of three biological replicates with three technical replicates each. See **Fig 8** for biological replicates in independent cell lines.

Figure 2. DUX4 transcriptional activity is not necessary for ISG suppression, whereas the C-terminal domain (CTD) is both necessary and sufficient.

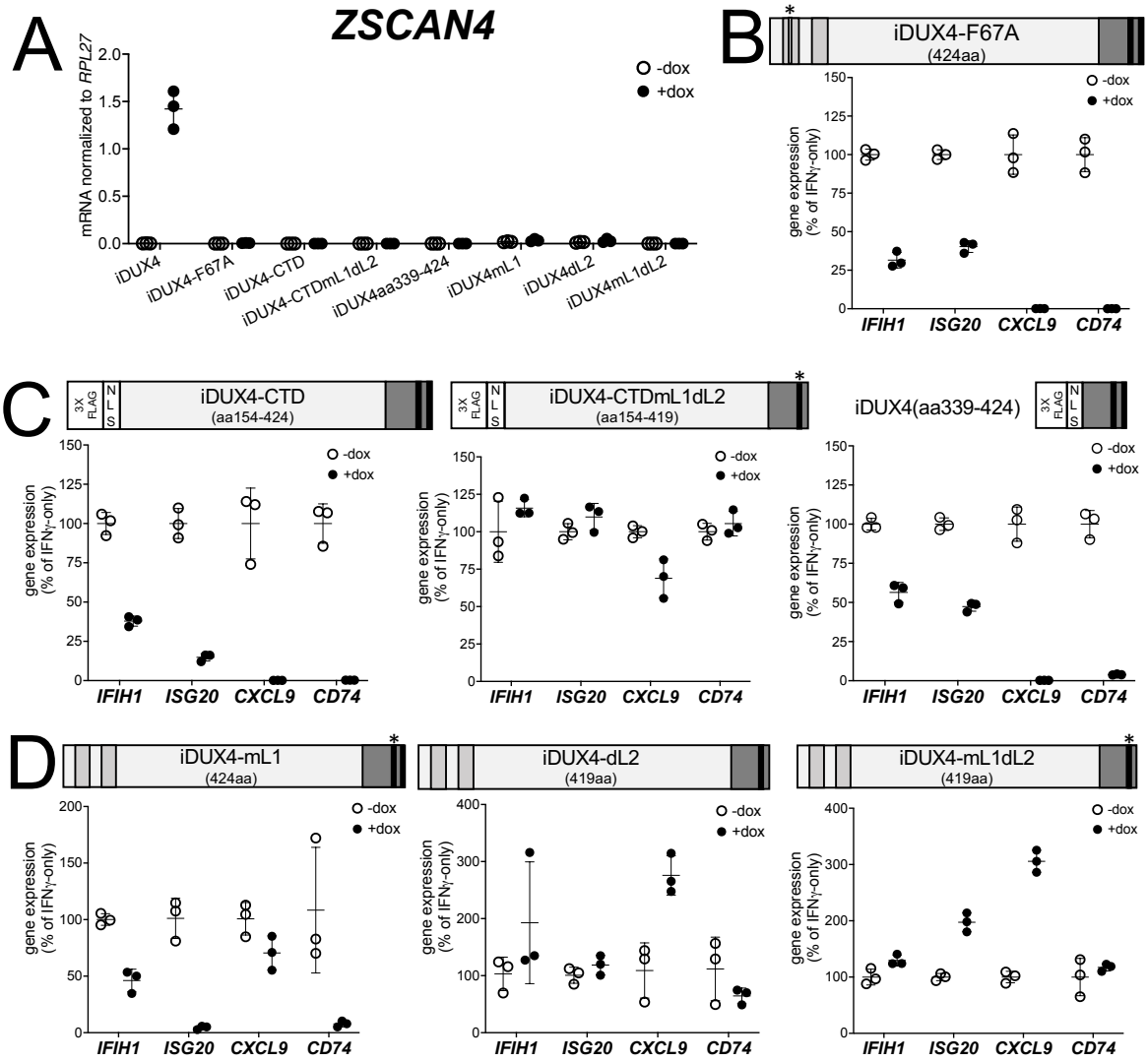

(**A**) MB135 cell lines with the indicated doxycycline inducible transgene ±doxycycline, were evaluated for *ZSCAN4* expression by RT-qPCR as a measure of the ability of the construct to activate a DUX4-target gene. Ct values were normalized to the housekeeping gene *RPL27*. Data represent the mean ±SD of three biological replicates. (**B-D**) MB135 cell lines with the indicated doxycycline inducible transgene were treated with IFNγ ±doxycycline. RT-qPCR was used to

evaluate expression of *IFIH1*, *ISG20*, *CXCL9*, and *CD74* and Ct values were normalized to the housekeeping gene *RPL27*, then normalized to the IFNγ-only treatment to set the induced level to 100%. Data represent the mean ±SD of three biological replicates with three technical replicates each. Light gray, homeodomains; medium gray, conserved region of CTD; black, (L)LxxL(L) motifs; * indicates sites of mutation for F67A in HD1 and mutation of first LLDELL to AADEAA. **See Fig 8** for additional cell lines.

Figure 3. The DUX4 protein interacts with STAT1 and additional immune response regulators.

Rank	Gene	Sum of PSMs	Max Unique Peptides
1	DDX3X	75	17
2	STAT1	43	7
3	PRKDC	39	17
4	YBX1	35	4
5	HNRNPM	35	14
6	HNRNPK	31	7
7	PPP2R1A	28	10
11	PABPC1	21	5
13	NCL	16	7
14	CDK4	16	5
20	HNRNPU	14	7
22	TRIM28	12	4

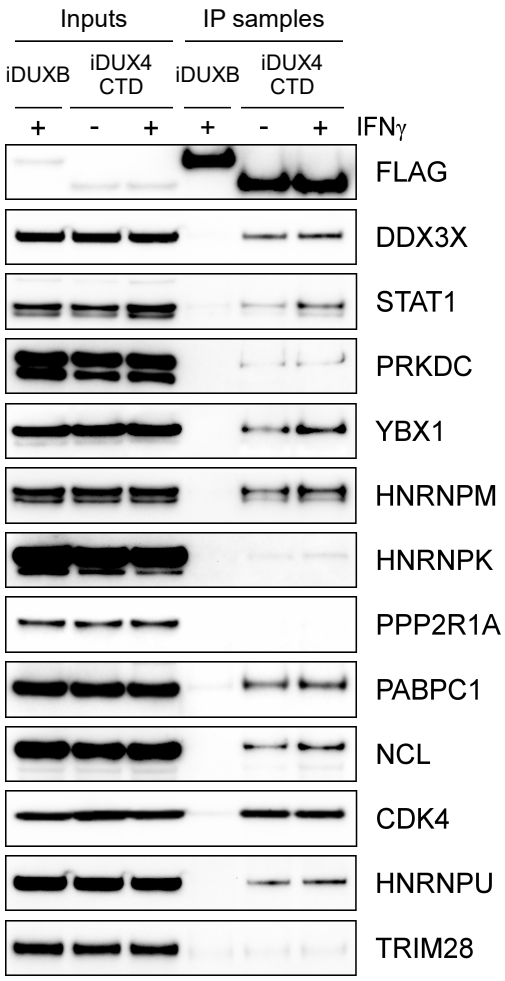

Left panel, representative candidate interactors identified by mass spectrometry of proteins that co-immunoprecipitated with the DUX4-CTD and their relative ranking in the candidate list (see **Table 2** for full list). Right panel, validation western blot of proteins that co-immunoprecipitate with the DUX4-CTD in cell lysates from MB135 cells expressing doxycycline-inducible 3xFLAG-DUXB or 3xFLAG-DUX4-CTD, ±IFNγ treatment.

Figure 4. The DUX4-CTD preferentially interacts with pSTAT1-Y701.

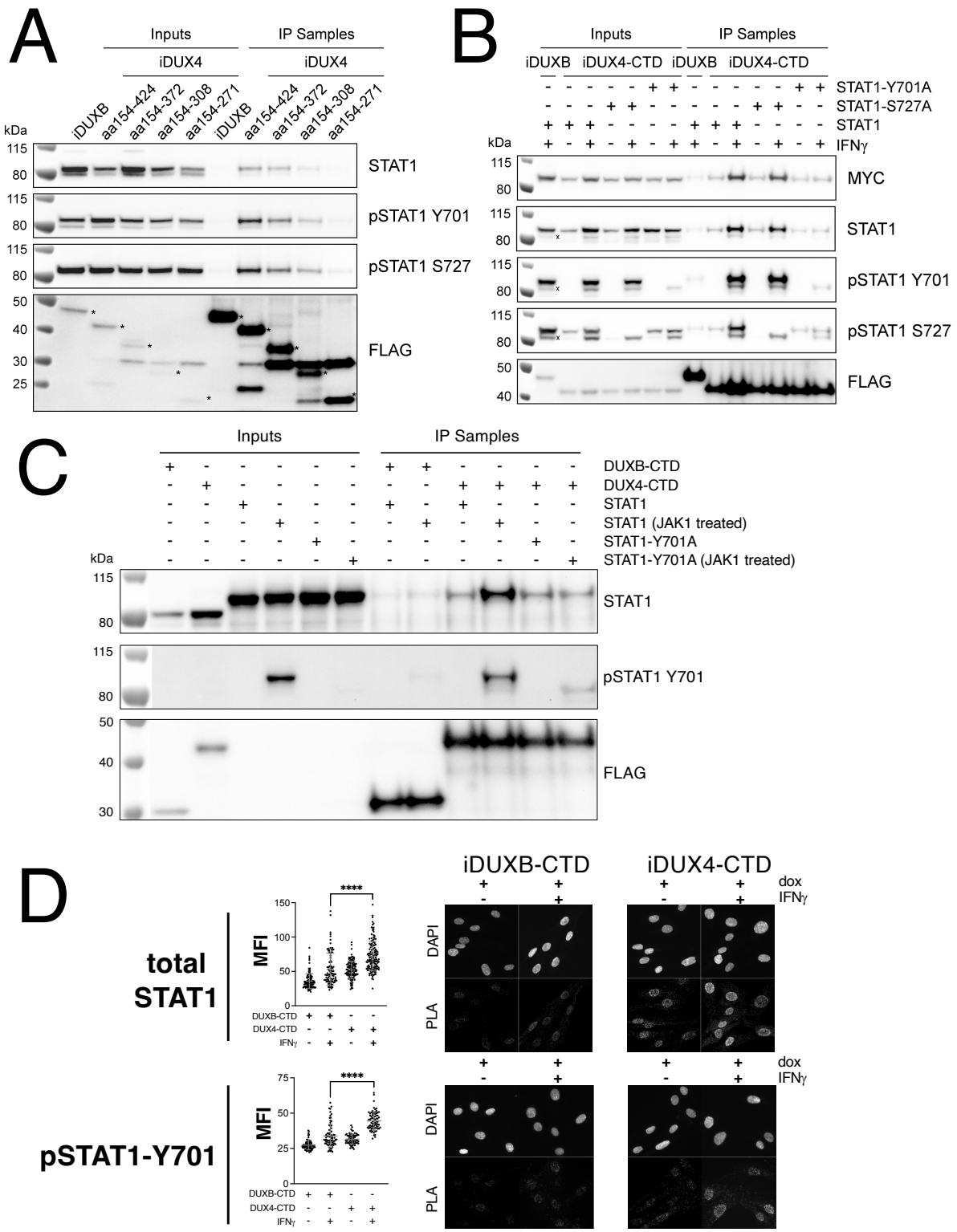

(**A**) Western blot showing input and immunoprecipitated proteins from either 3xFLAG-iDUXB (DUXB) or a truncation series of the 3x-FLAG-iDUX4-CTD cells (iDUX4) precipitated with anti-FLAG and probed with the indicated antibodies. Serial deletions of the iDUX4-CTD were assayed as indicated. All samples were treated with IFNγ. An asterisk indicates the correct band for each FLAG-tagged construct. (**B**) Input and anti-FLAG immunoprecipitation from 3xFLAG-iDUXB or 3x-FLAG-iDUX4-CTD cells co-expressing doxycycline inducible 3xMYC-iSTAT1, -iSTAT1-Y701A, or -iSTAT1-S727A with or without IFNγ treatment and probed with the indicated antibodies. An "x" indicates the endogenous (non-MYC tagged) STAT1 band. (**C**) Input and anti-FLAG immunoprecipitation from *in vitro* translated DUXB-CTD or DUX4-CTD proteins (both 3xFLAG-Tagged) that were incubated with *in vitro* translated MYC-Tagged STAT1 or STAT1-Y701 ±JAK1 treatment, probed with the indicated antibodies. (**D**) Proximity-ligation assay (PLA) showing co-localization of endogenous STAT1 and pSTAT1 Y701 with the iDUX4-CTD compared to the interaction with the DUXB-CTD, in the nuclear compartment of IFNγ- and doxycycline-treated MB135 cells. Mean fluorescent intensity (MFI) of the nuclei in the PLA channel was measured for 10 images per cell line and treatment and plotted (**** $p<0.0001$, unpaired t-test).

Figure 5. The DUX4-CTD decreases STAT1 occupancy at ISG promoters and blocks Pol-II recruitment.

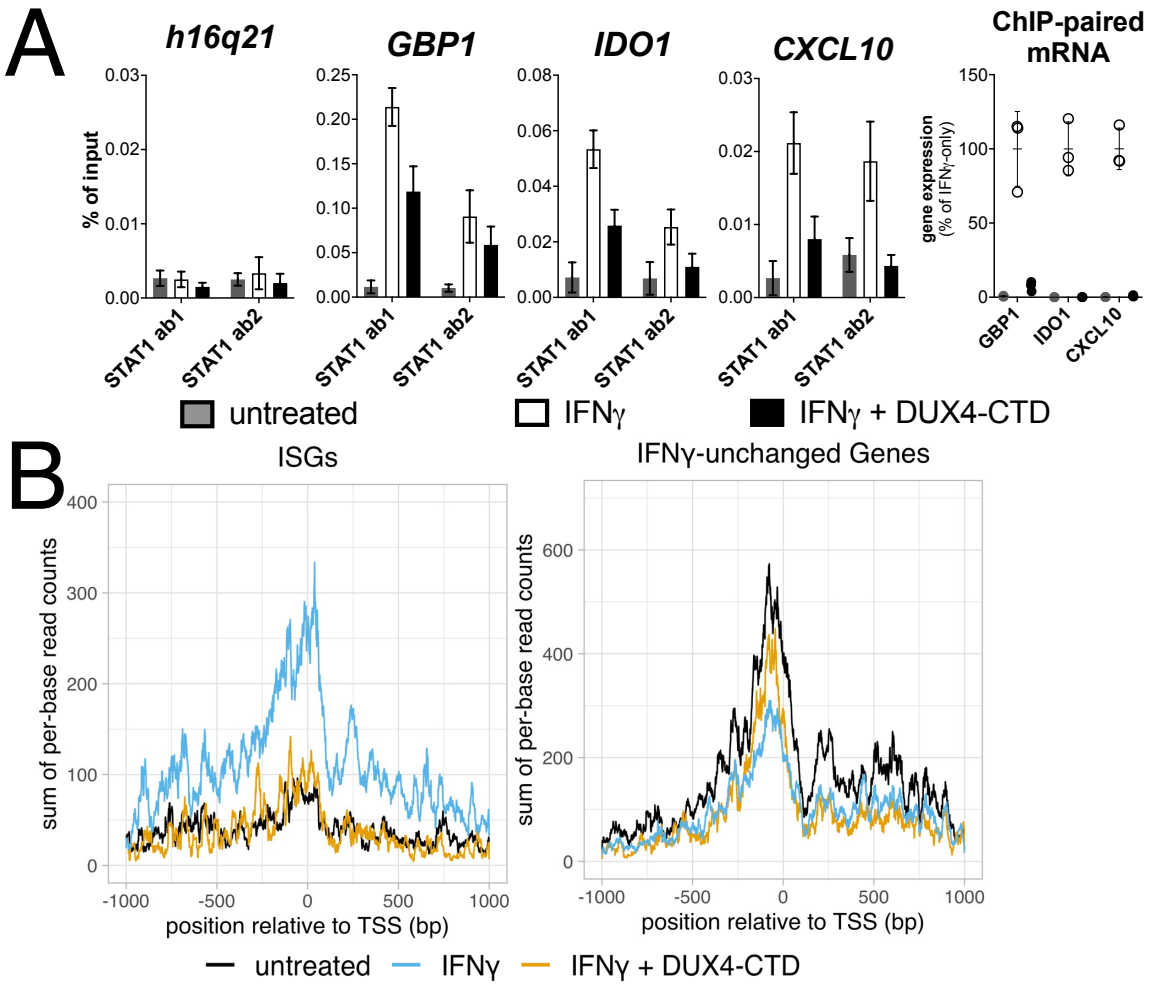

(**A, left four panels**) Chromatin immunoprecipitation using anti-STAT1 or IgG from MB135-iDUX4-CTD cells untreated, IFNγ-treated, or IFNγ and doxycycline treated. Ab1: 50:50 mix of STAT1 antibodies Abcam ab239360 and ab234400; Ab2: Abcam ab109320. ChIP-qPCR analysis relative to a standard curve constructed from purified input DNA was used to determine the quantity of DNA per IP sample, which was then graphed as a percent (%) of input (**** $p < 0.0001$, *** $p < 0.001$, ** $p < 0.005$, ns = not significant, unpaired t-test). Data represent the mean ±SD of two biological replicates with 3 technical replicates each. (**A, right panel**) RT-

qPCR of RNA from cells used for STAT1 ChIP showing induction of ISGs by IFNγ and suppression by DUX4-CTD. (**B**) CUT&Tag data showing the intensity of Pol-II signal across a 2000bp window centered on the TSS of ISGs (left) or IFNγ-unchanged genes (right) in untreated, IFNγ-treated, or IFNγ and doxycycline treated MB135-iDUX4-CTD cells.

Figure 6. Endogenous DUX4 suppresses ISG induction in FSHD muscle cells and in a sarcoma cell line expressing a CIC-DUX4 fusion gene.

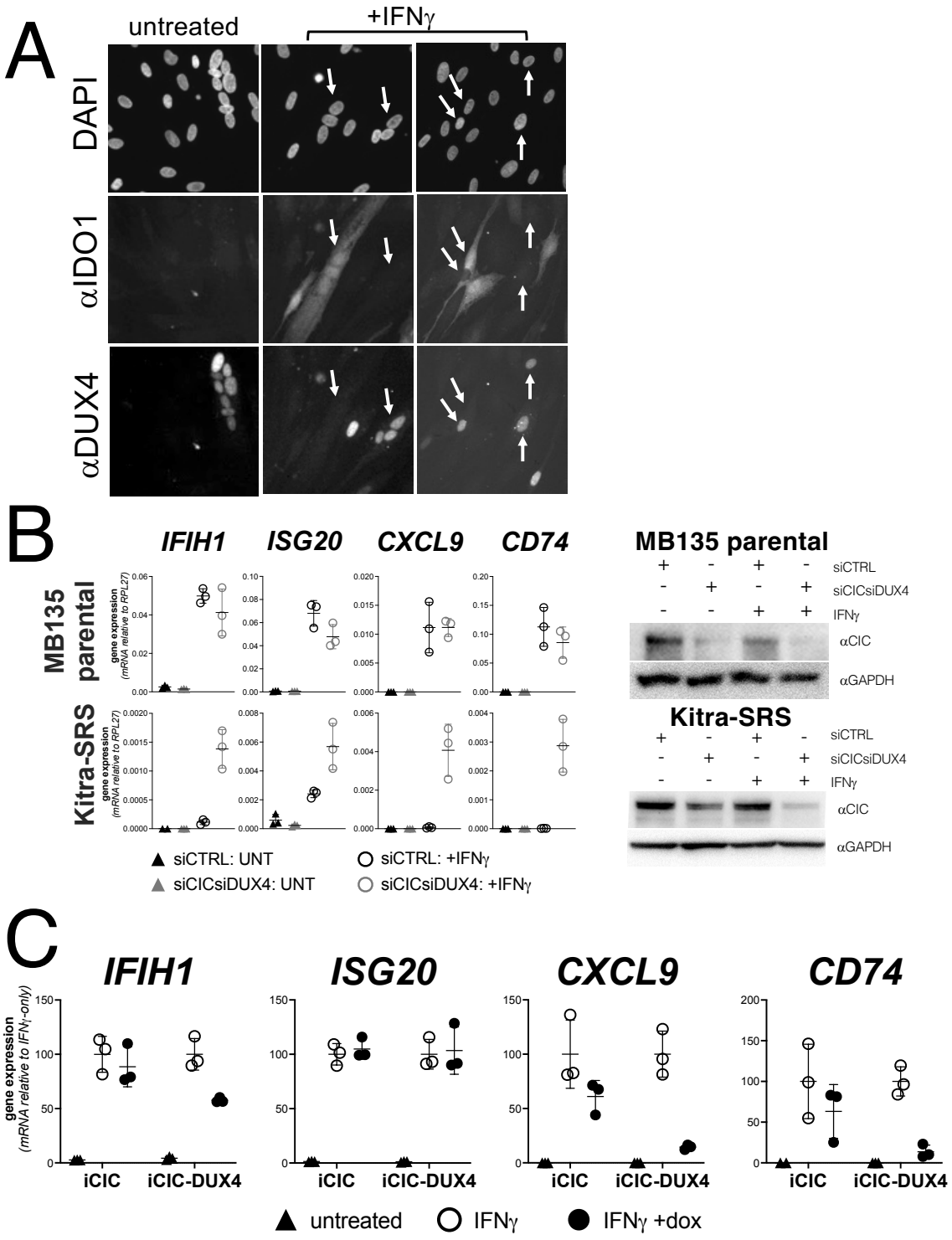

(**A**) FSHD MB200 myoblasts were differentiated into myotubes, which results in the expression of endogenous DUX4 in a subset of myotubes. Cultures were treated ±IFNγ, and DUX4 and IDO1 were visualized by immunofluorescence. A representative image of DUX4+ and DUX4- myotubes shows IDO1 induction only in the DUX4- myotubes (arrows). (**B, left panel**) RT-qPCR of the indicated genes in MB135 parental or Kitra-SRS that express a CIC DUX4-fusion gene containing the DUX4 CTD. Cells were transfected with control or CIC- and DUX4-targeting siRNAs. Ct values were normalized to the house-keeping gene *RPL27.* Data represent the mean ±SD of three biological replicates with three technical replicates each. (**B, right panel**) Western blot showing lysates from MB135 or Kitra-SRS cells treated with control or CIC- and DUX4-targeting siRNAs ±IFNγ and probed with the indicated antibodies. (**C**) RT-qPCR of the indicated genes in MB135 with an inducible CIC (MB135-iCIC) or an inducible CIC-DUX4 fusion gene (MB135-iCIC-DUX4). Cells were untreated, IFNγ-treated, or IFNγ and doxycycline treated. Ct values were normalized to the housekeeping gene *RPL27*, then normalized to the IFNγ-only treatment to set the induced level to 100%. Data represent the mean ±SD of three biological replicates with three technical replicates each.

Figure 7. Conservation of ISG repression and STAT1 interaction in mouse Dux.

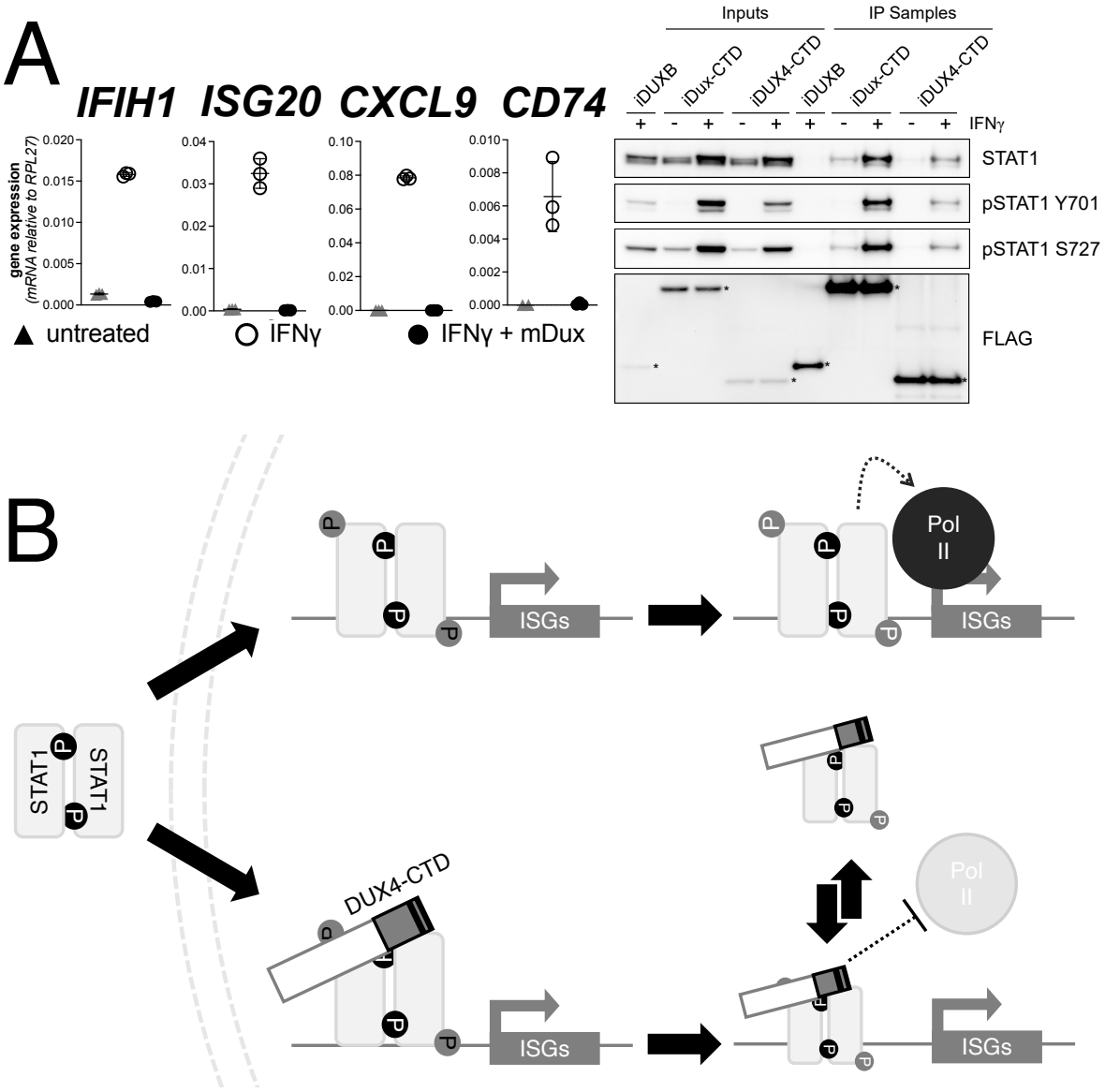

(**A, left panel**) RT-PCR of the indicated genes in MB135-iDux cells untreated or treated with IFNγ ±doxycycline. Ct values were normalized to the housekeeping gene *RPL27*, then normalized to the IFNγ-only treatment to set the induced level to 100%. Data represent the mean ±SD of three biological replicates with three technical replicates each. (**A, right panel**) Western blot showing input and immunoprecipitated proteins from either 3xFLAG-iDux or 3x-FLAG-

iDUXB cells ±IFNγ precipitated with anti-FLAG and probed with the indicated antibodies. (**B**) A model supported by the data showing how the DUX4-CTD might prevent STAT1 ISG induction. (Top) In the absence of the DUX4-CTD, pSTAT1 Y701 (black "P") dimerizes, translocates to the nucleus, binds its GAS motif in the ISG promoter, acquires secondary phosphorylation at S727 (grey "P"), and recruits a stable transcription complex that includes Pol II to drive transcription of ISGs. (Bottom) In the presence of the DUX4-CTD, STAT1 is phosphorylated, translocates to the nucleus, binds its GAS motif as evidenced by the pSTAT1 S727 in complex with the CTD, but diminished steady-state occupancy of STAT1 at the ISG promoters and absence of Pol-II recruitment indicate that the DUX4-CTD does not form a stable DNA bound complex associated with the recruitment of Pol-II and the pre-initiation complex. The (L)LXXL(L) motifs (black bars in DUX4-CTD) are necessary to interfere with transcription suppression and likely prevent STAT1 from interacting with a factor in the pre-initiation complex or by recruiting a co-repressor.

Figure 8. Transgene diagrams.

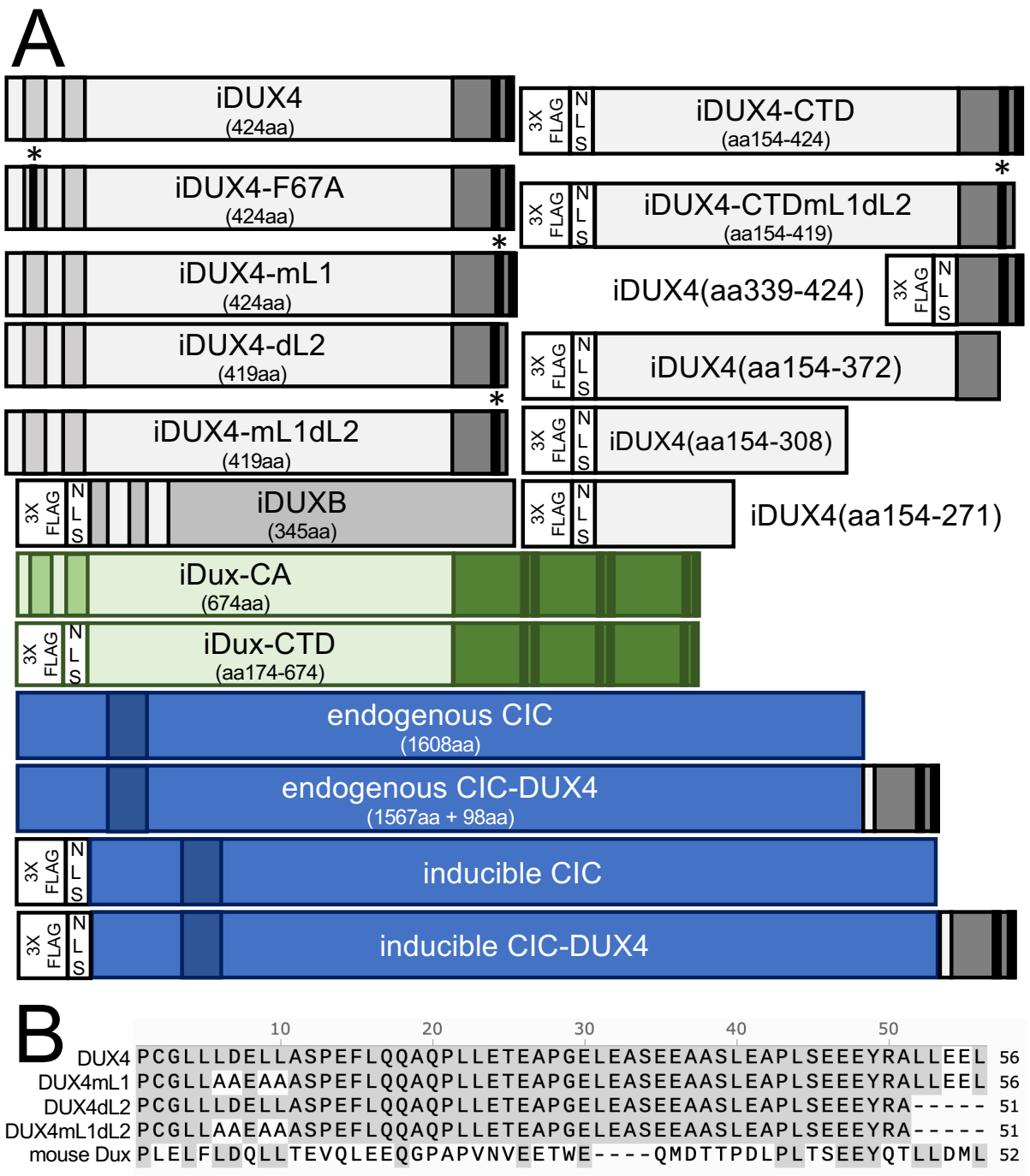

(**A**) Schematic depiction of each transgene used in this study highlighting the N-terminal homeodomains (light grey in DUX4, no fill in DUXB, light green in mDux), DNA-binding HMG box (dark blue in CIC and CIC-DUX4), conserved C-terminal domain (medium grey in

DUX4 and CIC-DUX4, medium green in mouse Dux), (L)LxxL(L) (black in DUX4 and CIC-DUX4, dark green in mouse Dux), mutations (* and black bar F67A, * replacement of (L)LxxL(L) with AADEAA), and 3xFLAG-NLS cassette regions (no fill). (**B**) MUSCLE alignment of the terminal ~50aa of the human DUX4, mutated human DUX4 (mL1, dL2, mL1dL2), and mouse Dux constructs used in this study.

Figure 9. Biological replicates in independent cell lines for each DUX4 construct.

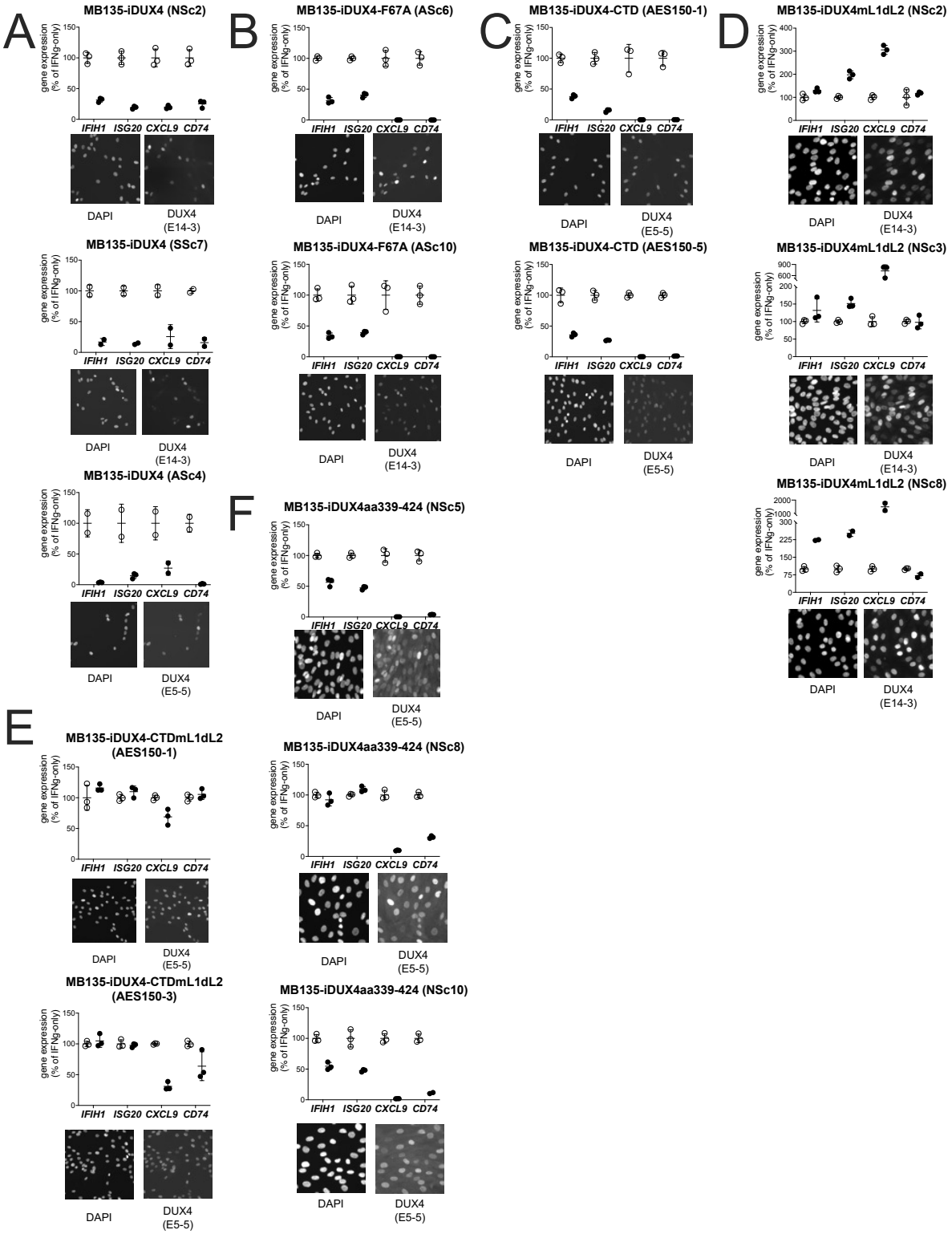

Additional subcloned MB135 cell lines of the iDUX4 (**A**), iDUX4-F67A (**B**), iDUX4-CTD (**C**), iDUX4mL1dL2 (**D**), iDUX4-CTDmL1dL2 (**E**), iDUX4aa339-324 (**F**) treated with IFNγ ±doxycycline. RT-qPCR shows ISG expression graphed as a % of IFNγ-only. Immunofluorescence panels show protein expression and nuclear localization using an antibody against the N-terminal (E14-3) or C-terminal (E5-5) residues of DUX4 as appropriate for the construct.

Figure 10. Expression of the DUX4-CTD does not prevent translocation of STAT1 to the nucleus.

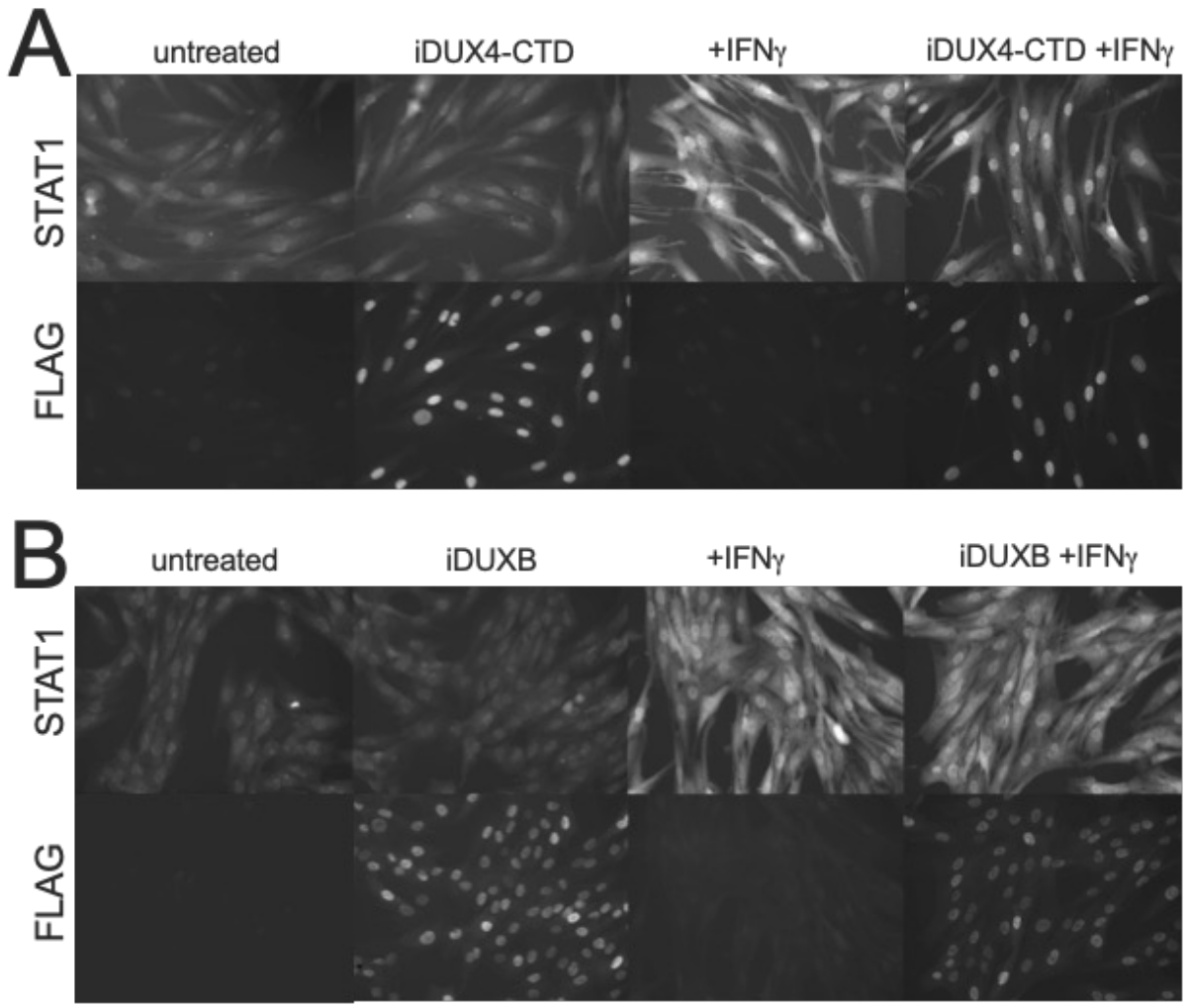

MB135-iDUX4-CTD (**A**) and MB135-iDUXB (**B**) cells were left untreated, treated with doxycycline, treated with IFNγ, or treated with combination doxycycline/IFNγ, then fixed and stained for STAT1 and either transgene. Both cell lines show good induction and nuclear translocation of STAT1 with IFNγ, with or without doxycycline-induction of the transgene.

Figure 11. Mouse Dux contains a triplication of the (L)LxxL(L)-containing region.

(**A**) Mouse Dux protein sequence with homeodomains in bold and (L)LxxL(L) motifs underlined. (**B**) Alignment of a partial triplication of the mouse Dux protein with aa258-440 aligning with aa441-623 and aa624-650 aligning with aa258-284.

Chapter 3: The effect of Human DUX4 and mouse Dux on induction of ISGs by Type-I IFN, dsDNA, and dsRNA.

This chapter contains unpublished work.

3.1 Introduction

The innate immune response is a cell's first line of direct defense against viruses, bacteria, and other pathogens. Innate immunity relies on recognition of Pathogen-Associated Molecular Patterns (PAMPs) to induce transcription of pro-inflammatory and anti-viral genes. Cytoplasmic nucleotides, such as the single-stranded (ss)RNA (ssRNA), double-stranded RNA (dsRNA), or double-stranded DNA (dsDNA) that can encode specific PAMP motifs within viral genomes, are one example of a PAMP. The canonical innate immune response to cytoplasmic double-stranded RNA (dsRNA) begins with binding to either retinoic acid-inducible gene-I (RIG-I) or melanoma differentiation-associated gene 5 (MDA5, also called IFIH1), depending on the length and modifications on the dsRNA. Short dsRNA with a exposed 5'-triphosphate group are sensed and bound by RIG-I, but longer dsRNA such as poly(I:C) and long dsRNA motif secondary structures within viral RNA are sensed and bound by MDA5. RNA binding by the RLRs induces their hydrolysis of ATP and a conformation change that facilitates their multimerization and interaction with the mitochondrial anti-viral signal (MAVS) adaptor protein that then directs the downstream activation of the TBK1 protein kinase, and phosphorylation and nuclear shuttling of the transcription factor IRF3. Similarly, binding of dsDNA to the sensor cGAS triggers production of cyclic guanosine monophosphate-adenosine monophosphate (cGAMP), which binds and activates STING, leading again to activation of TBK1 and IRF3. Both pathways can also result in phosphorylation and degradation of the NF-κB inhibitor IκB, freeing NF-κB to translocate to the nucleus. These transcription factors directly induce an early wave of immune genes via IRF3 activation, which includes the type I and III IFNs. Expression and secretion of the type-I interferons α and β (IFNα and IFNβ) then initiate ISG transcription via a complex of STAT1/STAT2/IRF9 or, to a lesser extent, the same STAT1 homodimer as

IFNγ. Because of my results showing that DUX4 could block the transcriptional response to IFNγ, I decided to test the ability of DUX4 to block the response to these other innate immune stimuli.

Additionally, because mouse Dux had such a strong effect on the transcriptional response to IFNγ in human myoblasts, I decided to test the conservation of this suppression in a mouse-in-mouse context using the murine myoblast C2C12 cell line. Mammals have a conserved core of ISGs comprising a mammalian 'interferome', as well as lineage-specific ISGs shaped by the evolutionary arms-races between those species and their unique pathogens[88-90]. The structure of IFNb and IFNγ as well as their receptors and downstream signaling components are well-characterized in mouse, allowing interrogation of the effect the mDux ortholog has on downstream immune signaling.

3.2 Results

3.2.1 DUX4 blocks the transcriptional response to multiple innate immune stimuli

To determine whether DUX4 also blocks ISG induction through these signaling pathways, I transfected the MB135-iDUX4 cells with three different innate immune stimuli: poly(I:C), a long dsRNA mimic to stimulate MDA5; RIG-I ligand, a short dsRNA with a 5'-ppp to stimulate DDX58; or cGAMP, a signaling component of the cGAS dsDNA sensing pathway. Additionally, I stimulated the cells with interferon-beta (IFNβ, Type-I interferon), which primarily signals through JAK-STAT pathways. For all signaling pathways, DUX4 suppressed the induction of a subset of the panel of ISGs (**Fig 12**) One exception, *CXCL9* was induced by IFNβ, poly(I:C), and the RIG-I ligand but not suppressed by DUX4. cGAMP did not induce *CXCL9* or *CD74*, precluding evaluation of the role of DUX4 in regulating these ISGs. Because

these signaling pathways rely on distinct transcription factors, these data suggest that DUX4 might interfere with multiple signaling factors. I decided to focus further efforts on identifying the mechanism behind the suppression of IFNγ-mediated transcription, as this pathway was most broadly suppressed by DUX4.

3.2.2 DUX4 may block dsDNA sensing through a STAT-independent mechanism

The cytosolic nucleotide sensing pathways converge at two points: IRF3 activation/translocation, and activation of Type-I interferon genes. Previous work has shown that IRF3 translocation is not impeded by expression of a DUX4 transgene (Sean Shadle, unpublished). However, I wanted to test if the suppression we were seeing was due to interference with the early role of IRF3 and NF-κB, or the later role of JAK-STAT signaling. That is to say, I was curious if the suppression could be explained by interference with STAT1 alone, or if I could show an interaction with an upstream factor. I treated cells ±1μM ruxolitinib, a STAT inhibitor, for 24hr before additionally treating ±doxycycline and either poly(I:C) or cGAMP. While the ruxolitinib should suppress any STAT-dependent activation, additional suppression in +doxycycline/+ruxolitinib treatment should represent suppression of other transcription factors in the signaling cascade. While I observed no difference in gene activation by dsRNA for the +ruxolitinib/poly(I:C) and the +doxycycline/ruxolitinib/poly(I:C) conditions, I did observe an additional decrease in gene activation in the +doxycycline/ruxolitinib/cGAMP as compared to the +ruxolitinib/cGAMP (**Fig 13**). This suggests that the suppression of dsRNA-mediated ISG induction by DUX4 is STAT1-dependent. However, DUX4 could be inhibiting more than just the STAT-based response to dsDNA.

3.3 Discussion

In this chapter, I showed that DUX4 is capable of blocking multiple innate immune signaling pathways. I tested cells' responses to dsRNA (poly(I:C) and short 5'ppp dsRNA), dsDNA (cGAMP), and Type-I interferon (IFNβ) in the presence and absence of a DUX4 transgene. I showed that most genes activated by these disparate pathways are suppressed in the presence of DUX4. Because the Type-I IFN, dsRNA, and dsDNA signaling pathways rely on distinct transcription factors, these data suggest that DUX4 might interfere with multiple signaling factors.

The experiments conducted in this body of research relied on a single 16h timepoint to evaluate the blockage of each pathway. Unfortunately, for the dsRNA and dsDNA-stimulated cells this would be ample time to induce an initial wave of ISGs and produce Type-I IFN, leading to a robust secondary induction of ISGs that was partially STAT1-dependent. Thus, the above work cannot specifically show that dsDNA or dsRNA sensing is impaired – it could be that STAT1 function is impaired in this downstream wave of gene activation, leading to our phenotype. While I conducted an initial experiment using ruxolitinib, a STAT inhibitor, that I believe showed a potential STAT-independent inhibition of the innate immune response to dsDNA, further work incorporating multiple earlier timepoints that can separate the dsRNA/dsDNA signaling pathways from their secondary activation of IFNα and IFNβ might reveal whether there is a distinct mechanism blocking these pathways, or if it is simply another manifestation of interference with STAT1. For instance, DUX4 could be inhibiting an early component of the cGAS/STING signaling pathway, which is specific to the dsDNA-sensing, rather than either TBK1 or IRF3, which are common to dsRNA and dsDNA sensing pathways.

Use of a STAT1-knockout cell line or direct observation of the activation and shuttling of the NF-κB and IRF transcription factors might shed light on this mechanism.

3.4 Materials and Methods

Multi-Pathway Immune Stimuli

Myoblasts were induced with 1 μg/mL of doxycycline (Sigma) for 4 hours prior to other treatments for a total of 20 hrs. For immune stimulation, cells were transfected with either (final concentrations) 10 μM 2',3'-cGAMP (Sigma Aldrich), 2 μg/mL poly(I:C) (Invitrogen), or 1 μg/mL 3'ppp-dsRNA RIG-I ligand (Dan Stetson Lab, UW) using Lipofectamine 2000 according to manufacturer's protocol, or were stimulated with 1000U IFNβ (PeproTech) by addition directly to cell culture medium. After 16 hours of immune stimulation, RNA was collected from cells using the NucleoSpin RNA Kit (Macherey-Nagel) according to manufacturer's instructions.

JAK-STAT Inhibitor Ruxolitinib

MB135 myoblasts with a doxycycline-inducible DUX4 transgene were untreated or treated with 1μM of the JAK-STAT inhibitor ruxolitinib for 24 hours, then were treated ±1μg/mL doxycycline for 4 hours before finally being treated either ±2μg/mL poly(I:C) or ±10μM 2',3'-cGAMP for 16 hours. RNA was collected from cells using the NucleoSpin RNA Kit (Macherey-Nagel) according to manufacturer's instructions.

cDNA Synthesis and RT-qPCR

All mRNA samples were quantified by nanodrop and 1 μg of RNA per sample was treated with DNase I Amplification Grade (Thermo Fisher), and then synthesized into cDNA using the Superscript IV First-Strand Synthesis System, including oligo dT primers (Invitrogen). qPCR was run in 384-well plates on an Applied Biosystems QuantStudio 6 Flex Real-Time PCR System (ABI) and analyzed in Microsoft Excel.

Figure 12. DUX4 suppresses induction of ISGs by Type-I IFN, dsDNA, and dsRNA.

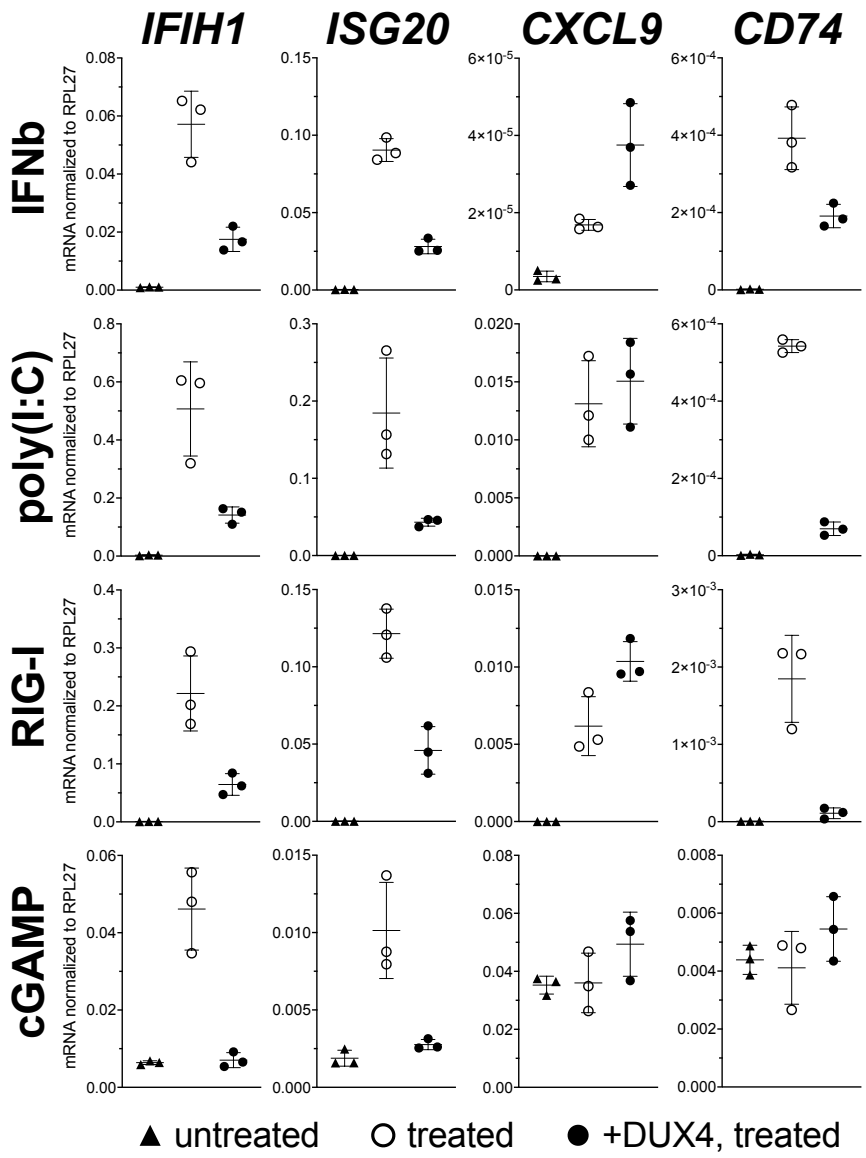

MB135-iDUX4 cells were untreated, treated with either IFNβ (Type-1 IFN pathway), poly(I:C) (IFIH1/MDA5 pathway), RIG-I ligand (DDX58/RIGI pathway), or cGAMP (cGAS/STING pathway), or treated with doxycycline and the same immune reagent. RT-qPCR was used to evaluate expression of *IFIH1*, *ISG20*, *CXCL9*, and *CD74*. Ct values were normalized to the housekeeping gene *RPL27*. Data represent the mean ±SD of three biological replicates with three technical replicates each.

Figure 13. DUX4 may inhibit dsDNA sensing through a STAT-independent mechanism.

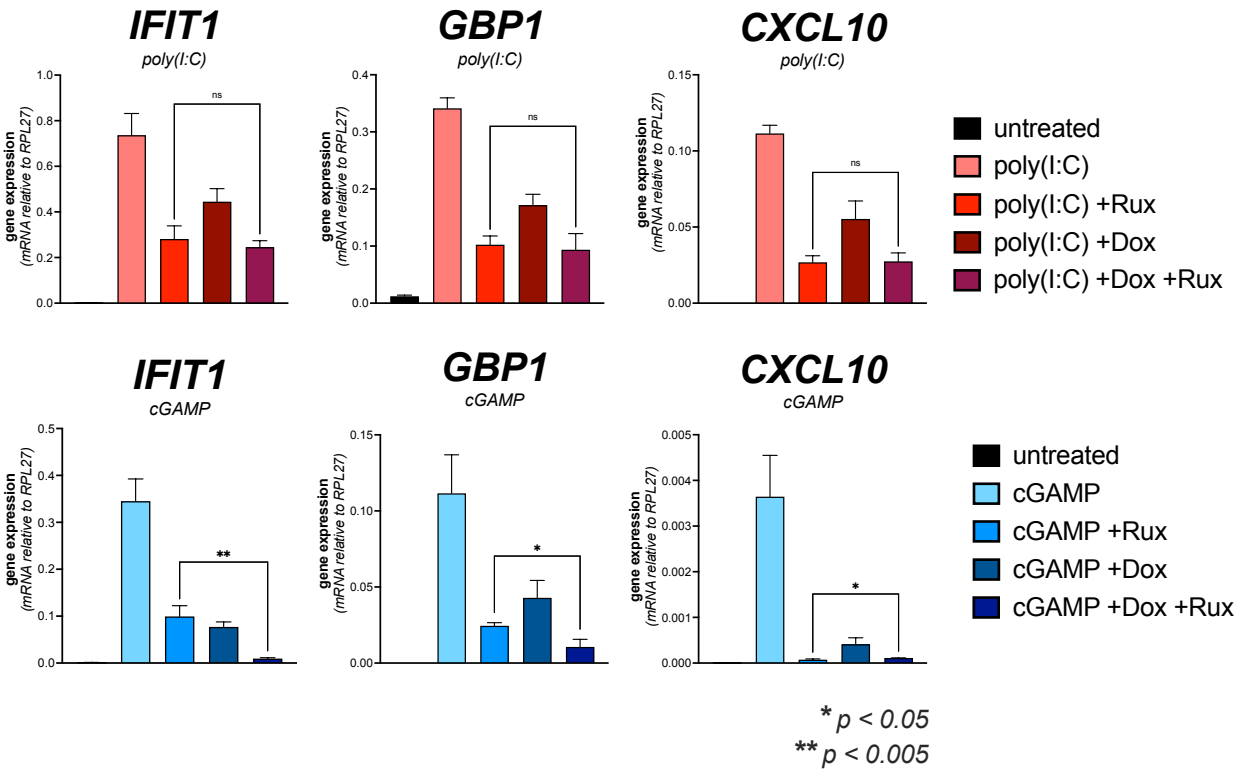

MB135 myoblasts with a doxycyline-inducible DUX4 transgene were untreated or treated with the JAK-STAT inhibitor ruxolitinib for 24 hours, then were treated ±doxycycline to induce transgenes and then stimulated with either poly(I:C) (a long dsRNA mimic) or cGAMP (a component of the cGAS/STING sensing pathway). RT-qPCR was used to evaluate expression of *IFIT1*, *GBP1*, and *CXCL10*. Ct values were normalized to the housekeeping gene *RPL27*. Data represent the mean ±SD of three biological replicates with three technical replicates each.

Chapter 4. DDX3X and the ISG response to dsRNA.

This chapter contains unpublished work.

4.1 Introduction

The human RNA helicase DEAD-box protein 3 (DDX3X) is expressed ubiquitously in tissues and plays several roles in innate immune signal transduction. There are two DDX3 genes, X and Y, which are located on the X and Y chromosomes, respectively, and thus are not fully redundant (XX individuals have two copies of DDX3X, and XY individuals have both DDX3X and DDX3Y). The myoblast cell line we use is derived from a patient with XX chromosomes, so I focus here on DDX3X. Following activation of the dsRNA sensing pathways, DDX3X is phosphorylated by IKKe and then acts as a scaffold to link IKKe and IRF3 to promote phosphorylation of IRF3, leading to induction of Type-I IFN [78, 79]. DDX3X is also directly recruited to the Type-I IFN promoter after phosphorylation by TBK1, where it promotes the recruitment of IRF3 and the p300/CBP co-activator complex [77, 91]. Finally, depletion of DDX3X in breast cancer cells has been shown to trigger accumulation of cytoplasmic dsRNAs and induction of Type-I IFN through the IFIH1/MDA5-mediated dsRNA sending pathway [92]. Thus, DDX3X is thought to be a positive mediator of dsRNA responses.

Our proteomics data showed that DDX3X co-immunoprecipitated with the DUX4-CTD, and this interaction was confirmed by Western blot analysis (**Fig 3**). As DDX3X is a positive regulator of the interferon response to dsRNA in other cell types, I decided to investigate A) its importance in the response to poly(I:C) in myoblasts, B) the potential conservation of this interaction with the mouse ortholog Dux, and C) what region of DDX3X is interacting with the DUX4-CTD.

4.2 Results

Initially, I used siRNAs targeting DDX3X to successfully knockdown the transcript in MB135 myoblasts, then treated with poly(I:C) and evaluated both knockdown efficiency and effect on two ISGs, *IFIH1* and *ISG20*, by RT-qPCR (**Fig 14**). I found that my knockdown was highly effective but had no effect on these two ISGs. Treatment with poly(I:C) seemed to slightly increase the expression of *DDX3X*, though not statistically significantly. I decided to expand my panel of ISGs to include *CXCL9* and *CD74* and sample protein as well for analysis by Western blot (**Fig 15**). This time, I found that RT-qPCR suggested a less efficient knockdown of *DDX3X*, and the protein was only reduced by 50%. Additionally, there was still no effect on the mRNA levels of *IFIH1* and *ISG20*, but a significant increase in *CXCL9* and *CD74* mRNA in the cells treated with siDDX3X compared to a non-targeting control siRNA. While the Western blot for IFIH1 was uninformative, the blot for ISG20 also appeared to show an increase in protein in the siDDX3X condition.

DDX3X was a putative interactor of the DUX4-CTD identified in our LC-MS screen, and the interaction was confirmed in lysate from MB135 cells using a Western blot. Thus, we wanted to test whether this interaction was conserved with the mouse ortholog Dux, as well as which segment of the protein was required for this interaction. To do so, we performed a fractionated IP on MB135 myoblasts expressing doxycycline-inducible 3XFLAG-DUXB, mouse 3XFLAG-Dux, or human 3XFLAG-DUX4, treated with doxycycline or doxycycline and IFNγ. We pulled down protein complexes with αFLAG and ran the lysates on a Western to probe for DDX3X. We saw that DDX3X, similar to STAT1, had an increased affinity for mouse Dux as compared to human DUX4, and there was no interaction with the DUXB negative control (**Fig 16**). Additionally, this interaction was not dependent on IFNγ treatment.

4.3 Discussion

In this section, I showed that *DDX3X* is expressed in MB135 myoblasts, increases slightly with poly(I:C) treatment, and can be efficiently knocked down using siRNAs. However, DDX3X is not required for the upregulation of ISGs *IFIH1* or *ISG20* in response to poly(I:C) in our myoblast cells. Knockdown of DDX3X may in fact facilitate greater expression of ISGs *CXCL9* and *CD74*. I also showed that another DUXC family member, mouse Dux, interacts with DDX3X in cell culture.

A remaining question is the importance of DDX3X for the dsRNA response in the presence of the DUX4-CTD. Especially considering that knockdown of DDX3X appears to upregulate the ISGs *CXCL9* and *CD74*, it could be interesting to conduct another siDDX3X experiment with untreated, poly(I:C)-treated, and doxycycline- and poly(I:C)-treated cells, to see if knockdown of DDX3X can relieve the inhibition of the IFIH1/MDA5 pathway by DUX4. If such a knockdown rescued the ISG response to poly(I:C) in DUX4-CTD expressing myoblasts, it could indicate a novel role for DDX3X in complex with DUX4 as an inhibitor that stifles ISG responses in myoblast cells.

4.4 Materials and Methods

siRNA treatment

MB135 cells were grown to 70% confluence in 6-well dishes then transfected with 50pmol total siRNAs (either non-targeting control or pool of 4 siDDX3X) using OptiMEM media and Lipofectamine RNAiMax according to the manufacturer's recommendations. Cells were left to sit for 24hr, then media was changed to fresh F10 and 2µg/mL poly(I:C) was added to appropriate wells. After 16 hours, RNA was collected from cells using the NucleoSpin RNA Kit (Macherey-Nagel) according to manufacturer's instructions and used to synthesize cDNA and run qPCR as previously described.

siRNA sequences for DDX3X (Dharmacon siON-TARGET*plus* pool of 4)

J-006874-06: CAGAUUUAGUGGAGGGUUU

J-006874-07: GCAACACUGGGAUUAAUUU

J-006874-08: GAUGCUGGCUCGUGAUUUC

J-006874-18: GGUAUUAGCACCAACGAGA

Antibodies

Antibodies against ISG20 [EPR8972] (ab166633), MDA5/IFIH1 [EPR6743] (ab126630), and

Figure 14. DDX3X knockdown by siRNA does not affect upregulation of ISGs in response to poly(I:C).

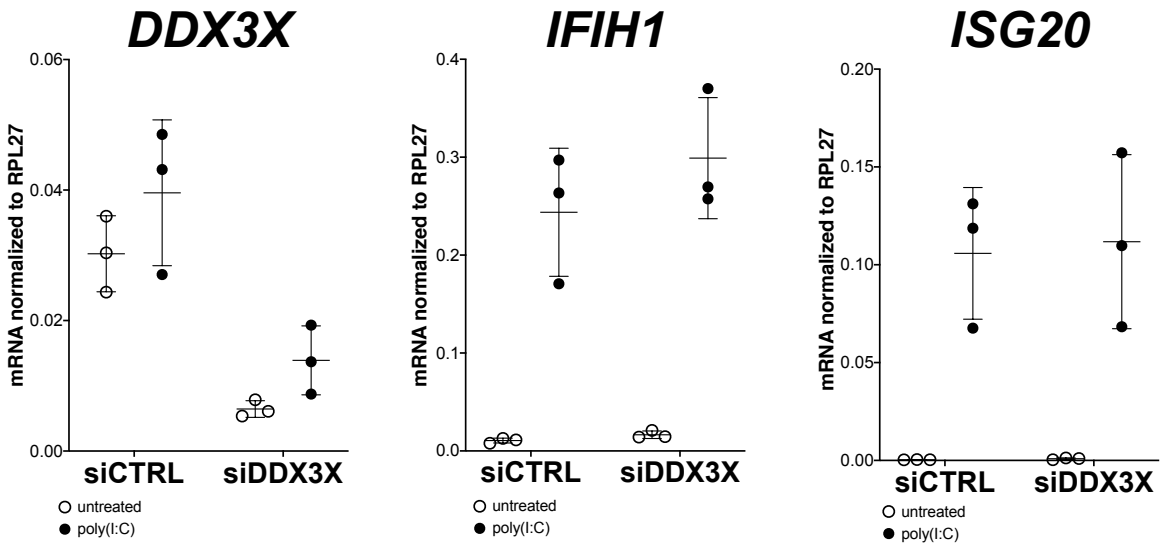

Following siRNA knockdown of *DDX3X* (left panel), MB135 myoblasts were treated ±poly(I:C) for 16 hours. RT-qPCR was used to evaluate mRNA levels of *IFIH1* and *ISG20*. Ct values were normalized to the housekeeping gene *RPL27*. Data represent the mean ±SD of three biological replicates with three technical replicates each.

Figure 15. siRNA knockdown of DDX3X may allow superinduction of some ISGs.

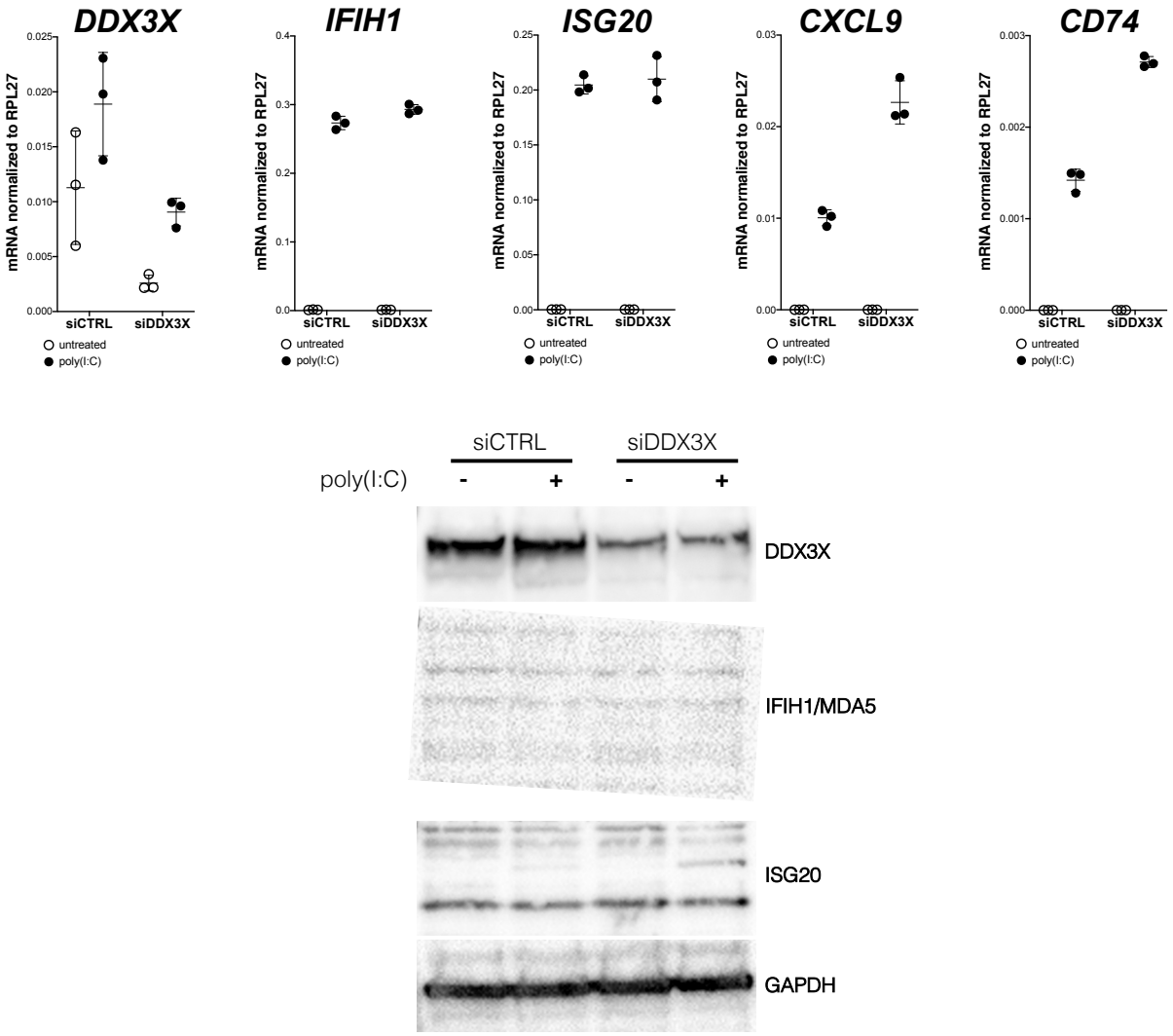

MB135 myoblasts were treated with siRNAs targeting *DDX3X*, then treated ±poly(I:C) for 16 hours. RT-qPCR was used to evaluate gene expression of *DDX3X*, *IFIH1*, *ISG20*, *CXCL9*, and *CD74* (top panels). Western blot was also used to evaluate protein levels of DDX3X, IFIH1, and ISG20, with GAPDH as a loading reference (bottom panels).

Figure 16. The interaction with DDX3X is conserved in mouse Dux.

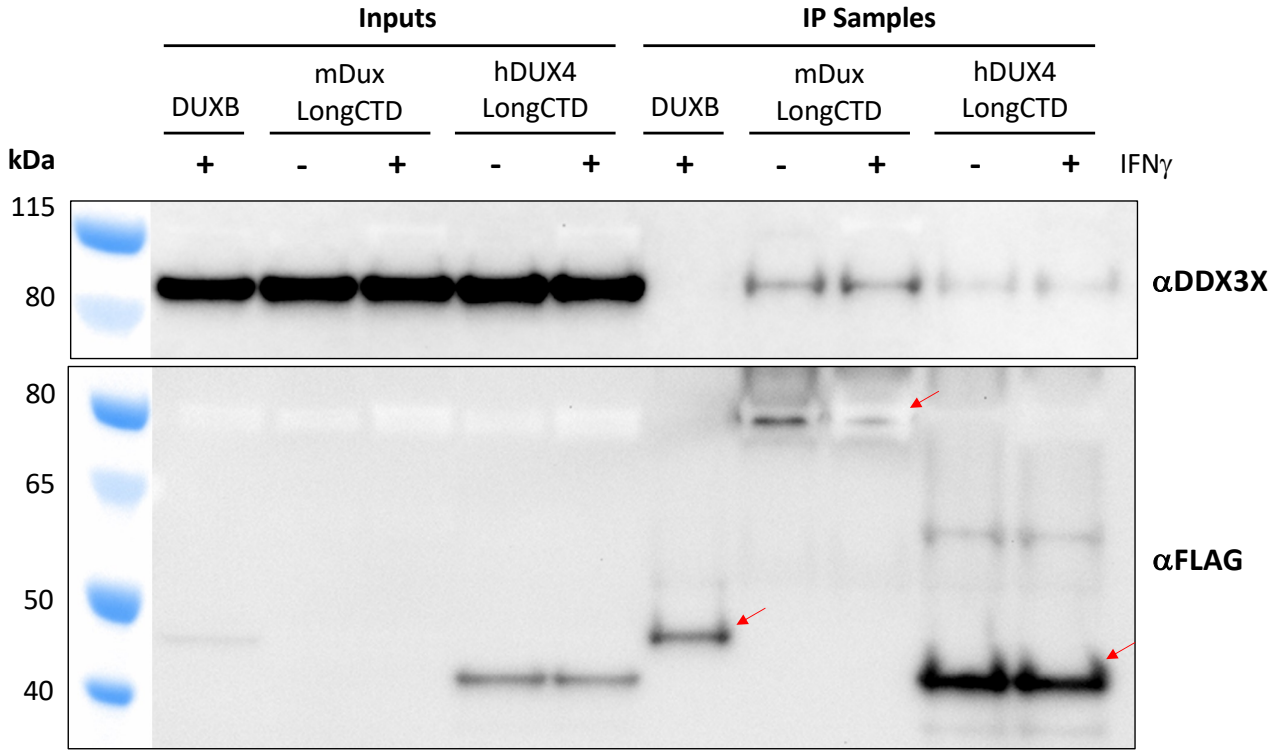

MB135 myoblasts with 3XFLAG-DUXB, 3XFLAG-mDux, or 3XFLAG-DUX4-CTD transgenes were treated with IFNγ ±doxycycline, then a fractionated nuclear IP was performed using the αFLAG antibody. Inputs and IP samples were run on a Western blot and probed with the indicated antibodies.

Chapter 5: Discussion

In my thesis work, I set out to characterize the effect of the transcription factor DUX4 on the JAK-STAT innate immune signaling pathway. When I initially began this project as a rotation student, we only knew that transduction of cell with lentivirus encoding DUX4 did not induce the expected upregulation of ISGs such as *IFIH1* and *ISG20* [22], and that the dsRNAs produced after prolonged DUX4 expression also did not lead to a transcriptional immune response, though they did activate the PKR-based apoptotic immune response pathway [83]. The finding that DUX4 robustly inhibited the transcriptional response to IFNγ grew into a multi-branched project that has implications for early human development, cancer, and muscular dystrophy.

My project showed the highly reproducible dampening effect that DUX4 has on innate immune signaling pathways. Cells which normally have a robust transcriptional response to IFNγ are silent in the presence of DUX4. A transcriptionally inactive carboxyterminal fragment of DUX4, the DUX4-CTD, is necessary and sufficient to broadly suppress ISG induction. The DUX4-CTD co-localizes with STAT1 in the nucleus, diminishes STAT1 occupancy at ISG promoter regions, and prevents recruitment of Pol-II and transcriptional machinery. Whereas two small (L)LXXL(L) motifs are necessary to suppress transcriptional activation by STAT1, they are not necessary for the interaction of the DUX4-CTD and STAT1. To expand these findings beyond cell culture overexpression systems, I showed that the same effect is achieved by endogenous expression of DUX4 in FSHD muscle cells or the CIC-DUX4 fusion protein in sarcoma cells. Finally, I showed that the mouse ortholog of DUX4, Dux, has a similar interaction with STAT1 and even more robustly suppresses the ISG response to IFNγ in human myoblast cells.

This final point, that suppression of the transcriptional immune response is conserved across DUXC family members, points to a broader potential role for these embryonic transcription factors in modulating the maternal-fetal immune interface. DUXC-family transcription factors are only found in placental mammals, where placental invasion of maternal tissue and evasion of the maternal immune response is a critical step in implantation and embryonic development. Both human DUX4 and mouse Dux are expressed at the cleavage stage of development, very early in embryogenesis; however, DUX4 has been shown to have long-lasting effects on chromatin, protein expression, and gene transcription [63, 64, 93]. Even if the initial burst of DUX4 is not potent enough to sustain suppression of local immune responses past implantation, Western blot and RT-PCR data from our lab has shown there is DUX4 expression in placental tissues themselves (Linda Geng, unpublished data). Further studies will need to focus on the effects of mouse Dux, canine DUXC, and other DUXC-family members on their own species' immune signaling cascades in order to pursue this tantalizing possibility of a conserved role in modulating maternal-fetal immune interactions.

Additionally, the suppression of local immune signaling by DUX4 raises several questions about the role of the innate immune response in FSHD. FSHD is a slow-developing disease characterized by rare bursts of toxic DUX4 expression in adult skeletal muscle that lead to cell death. Previous studies have struggled to identify biomarkers that can aid in early detection of FSHD; however, some studies suggest that genes associated with immune/inflammatory responses might be upregulated in and distinguish FSHD-positive muscle biopsy samples from controls [42, 43]. Immune responses are known to contribute to tissue growth and repair, including pruning of defective cells and promotion of regeneration in muscle. Thus, the sporadic endogenous expression of DUX4 in FSHD-affected muscles could contribute

to FSHD pathology by producing disordered or contradictory immune responses, impeding muscle repair, and contributing to a low-level, prolonged smoldering phenotype. Future studies investigating the effect of DUX4 on immune signaling in an intact muscle environment could contextualize my own findings significantly.

In addition to my main body of work, I also showed that DUX4 is capable of repressing the transcriptional response to Type-I interferon, dsRNA, and dsDNA stimuli. Type-I interferon responses canonically rely on a complex of STAT1, STAT2, and IRF9 to transcriptionally activate ISGs. While my work showed that this pathway is blocked, I left many mechanistic stones unturned. In the future it would be valuable to investigate whether DUX4 interacts with STAT1 downstream of Type-I interferon stimulus, if the STAT-IRF complex can form in the presence of DUX4, and if so whether this complex is still capable of binding chromatin. The dsRNA and dsDNA pathways rely on a separate set of transcription factors. In Chapter 3 I showed that pathways downstream of poly(I:C), RIG-I ligand, and cGAS are robustly blocked by DUX4 expression. However, I have not formally disentangled the direct induction of ISGs by dsRNA/dsDNA sensing components from the downstream activation of Type-I interferon by these pathways that leads to a secondary wave of ISG activation. A preliminary experiment with a JAK-STAT inhibitor suggested the interference with dsDNA sensing could be independent of or not solely due to interference with STAT1, but this is hardly definitive. Further experiments including multiple early timepoints, direct observation of the initial transcription factors in the dsRNA/dsDNA pathways (such as NF-κB and IRFs), and perhaps experiments conducted in STAT-knockout cell lines could all contribute significantly to our understanding of the mechanism of this blockage.

6. REFERENCES

1. Yang W, H.P., *Skeletal muscle regeneration is modulated by inflammation.* Journal of Orthopaedic Translation, 2018. **13**: p. 25-32.
2. Chazaud B, S.C., Lafuste P, Bassez G, Rimaniol AC, Poron F, Authier FJ, Dreyfus PA, Gherardi RK, *Satellite cells attract monocytes and use macrophages as a support to escape apoptosis and enhance muscle growth.* Journal of Cell Biology, 2003. **163**(5): p. 1133-1143.
3. Hawke TJ, G.D., *Myogenic satellite cells: physiology to molecular biology.* Journal of Applied Physiology, 2001. **91**(2): p. 534-551.
4. Gordon JR, G.S., *Mast cells as a source of both preformed and immunologically inducible TNF-alpha/cachectin.* Nature, 1990. **346**(6281): p. 274-276.
5. Fielding RA, M.T., Ding W, Fiatarone MA, Evans WJ, Cannon JG, *Acute phase response in exercise. III. Neutrophil and IL-1 beta accumulation in skeletal muscle.* American Journal of Physiology, 1993. **265**: p. 166-172.
6. Chen SE, G.E., Zhang Y, Zhan M, Mohan RK, Li AS, Reid MB, Li YP, *Role of TNF-{alpha} signaling in regeneration of cardiotoxin-injured muscle.* American Journal of Physiology, 2005. **289**(5): p. C1179-1187.
7. Chen SE, J.B., Li YP, *TNF-alpha regulates myogenesis and muscle regeneration by activating p38 MAPK.* American Journal of Physiology, 2007. **292**(5): p. C1660-1671.
8. Zhang J, X.Z., Qu C, Cui W, Wang X, Du J, *CD8 T cells are involved in skeletal muscle regeneration through facilitating MCP-1 secretion and Gr1(high) macrophage infiltration.* Journal of Immunology, 2014. **193**(10): p. 5149-5160.
9. Fu X, X.J., Wei Y, Li S, Liu Y, Yin J, Sun K, Sun H, Wang H, Zhang Z, Zhang BT, Sheng C, Wang H, Hu P, *Combination of inflammation-related cytokines promotes long-term muscle stem cell expansion.* Cell Research, 2015. **25**(6): p. 655-673.
10. Chew, G.-L., et al., *DUX4 Suppresses MHC Class I to Promote Cancer Immune Evasion and Resistance to Checkpoint Blockade.* Developmental Cell, 2019. **50**(5): p. 658-671.e7.
11. Sade-Feldman, M., et al., *Resistance to checkpoint blockade therapy through inactivation of antigen presentation.* Nature Communications, 2017. **8**(1): p. 1136.
12. Zaretsky, J.M., et al., *Mutations Associated with Acquired Resistance to PD-1 Blockade in Melanoma.* New England Journal of Medicine, 2016. **375**(9): p. 819-829.
13. Rapacz-Leonard, A., M. Dąbrowska, and T. Janowski, *Major histocompatibility complex I mediates immunological tolerance of the trophoblast during pregnancy and may mediate rejection during parturition.* Mediators Inflamm, 2014. **2014**: p. 579279.
14. Ellis, S.A., et al., *Evidence for a novel HLA antigen found on human extravillous trophoblast and a choriocarcinoma cell line.* Immunology, 1986. **59**(4): p. 595-601.
15. King, A., et al., *Surface expression of HLA-C antigen by human extravillous trophoblast.* Placenta, 2000. **21**(4): p. 376-87.
16. King, A., et al., *HLA-E is expressed on trophoblast and interacts with CD94/NKG2 receptors on decidual NK cells.* Eur J Immunol, 2000. **30**(6): p. 1623-31.
17. McCracken, S.A., E. Gallery, and J.M. Morris, *Pregnancy-Specific Down-Regulation of NF-κB Expression in T Cells in Humans Is Essential for the Maintenance of the Cytokine Profile Required for Pregnancy Success.* The Journal of Immunology, 2004. **172**(7): p. 4583-4591.

18. Ander, S.E., M.S. Diamond, and C.B. Coyne, *Immune responses at the maternal-fetal interface.* Sci Immunol, 2019. **4**(31).
19. Alijotas-Reig, J., E. Llurba, and J.M. Gris, *Potentiating maternal immune tolerance in pregnancy: A new challenging role for regulatory T cells.* Placenta, 2014. **35**(4): p. 241-248.
20. Warning, J.C., S.A. McCracken, and J.M. Morris, *A balancing act: mechanisms by which the fetus avoids rejection by the maternal immune system.* REPRODUCTION, 2011. **141**(6): p. 715-724.
21. McCracken, S.A., et al., *Pregnancy is associated with suppression of the nuclear factor kappa B/I kappa B activation pathway in peripheral blood mononuclear cells.* Journal of Reproductive Immunology, 2003. **58**(1): p. 27-47.
22. Geng, L.N., et al., *DUX4 activates germline genes, retroelements, and immune mediators: implications for facioscapulohumeral dystrophy.* Dev Cell, 2012. **22**(1): p. 38-51.
23. Choi, S.H., et al., *DUX4 recruits p300/CBP through its C-terminus and induces global H3K27 acetylation changes.* Nucleic Acids Res, 2016. **44**(11): p. 5161-73.
24. Kawamura-Saito, M., et al., *Fusion between CIC and DUX4 up-regulates PEA3 family genes in Ewing-like sarcomas with t(4;19)(q35;q13) translocation.* Hum Mol Genet, 2006. **15**(13): p. 2125-37.
25. Hendrickson, P.G., et al., *Conserved roles of mouse DUX and human DUX4 in activating cleavage-stage genes and MERVL/HERVL retrotransposons.* Nat Genet, 2017. **49**(6): p. 925-934.
26. Whiddon, J.L., et al., *Conservation and innovation in the DUX4-family gene network.* Nat Genet, 2017. **49**(6): p. 935-940.
27. De Iaco, A., et al., *DUX-family transcription factors regulate zygotic genome activation in placental mammals.* Nat Genet, 2017. **49**(6): p. 941-945.
28. Leidenroth, A. and J.E. Hewitt, *A family history of DUX4: phylogenetic analysis of DUXA, B, C and Duxbl reveals the ancestral DUX gene.* BMC Evol Biol, 2010. **10**: p. 364.
29. Chao-Jen Wong, J.L.W., Ashlee T Langford, Andrea E Belleville, Stephen J Tapscott, *Canine DUXC: implications for DUX4 retrotransposition and preclinical models of FSHD.* Human Molecular Genetics, 2022. **31**(10): p. 1694-1704.
30. Tawil, R., S.M. van der Maarel, and S.J. Tapscott, *Facioscapulohumeral dystrophy: the path to consensus on pathophysiology.* Skelet Muscle, 2014. **4**: p. 12.
31. Bakker E, W.C., Vossen R, Padberg GW, Hewitt J, van Der Wielen M, Rasmussen K, Frants RR, *The FSHD-linked locus D4F104S1 (p13E-11) ON 4q35 has a homologue on 10qter.* Muscle & Nerve, 1995. **18**(S13): p. S39-S44.
32. van Deutekom, J.C.T., et al., *Evidence for Subtelomeric Exchange of 3.3 kb Tandemly Repeated Units between Chromosomes 4q35 and 10q26: Implications for Genetic Counselling and Etiology of FSHD1.* Human Molecular Genetics, 1996. **5**(12): p. 1997-2003.
33. van der Maarel, S.M., et al., *De Novo Facioscapulohumeral Muscular Dystrophy: Frequent Somatic Mosaicism, Sex-Dependent Phenotype, and the Role of Mitotic Transchromosomal Repeat Interaction between Chromosomes 4 and 10.* The American Journal of Human Genetics, 2000. **66**(1): p. 26-35.

34. Salort-Campana, E., et al., *Low penetrance in facioscapulohumeral muscular dystrophy type 1 with large pathological D4Z4 alleles: a cross-sectional multicenter study.* Orphanet Journal of Rare Diseases, 2015. **10**(1): p. 2.
35. Larsen, M., et al., *Diagnostic approach for FSHD revisited: SMCHD1 mutations cause FSHD2 and act as modifiers of disease severity in FSHD1.* European Journal of Human Genetics, 2015. **23**(6): p. 808-816.
36. van den Boogaard, M.L., et al., *Mutations in DNMT3B Modify Epigenetic Repression of the D4Z4 Repeat and the Penetrance of Facioscapulohumeral Dystrophy.* Am J Hum Genet, 2016. **98**(5): p. 1020-1029.
37. Bouwman, L.F., et al., *Dnmt3b regulates DUX4 expression in a tissue-dependent manner in transgenic D4Z4 mice.* Skeletal Muscle, 2020. **10**(1): p. 27.
38. Statland, J.M. and R. Tawil, *Facioscapulohumeral Muscular Dystrophy.* Continuum (Minneap Minn), 2016. **22**(6, Muscle and Neuromuscular Junction Disorders): p. 1916-1931.
39. Goselink, R.J.M., et al., *Early onset facioscapulohumeral dystrophy - a systematic review using individual patient data.* Neuromuscul Disord, 2017. **27**(12): p. 1077-1083.
40. Frisullo, G., et al., *CD8+ T Cells in Facioscapulohumeral Muscular Dystrophy Patients with Inflammatory Features at Muscle MRI.* Journal of Clinical Immunology, 2011. **31**(2): p. 155-166.
41. Arahata, K., et al., *Inflammatory response in facioscapulohumeral muscular dystrophy (FSHD): Immunocytochemical and genetic analyses.* Muscle & Nerve, 1995. **18**(S13): p. S56-S66.
42. Wang, L.H., et al., *MRI-informed muscle biopsies correlate MRI with pathology and DUX4 target gene expression in FSHD.* Hum Mol Genet, 2019. **28**(3): p. 476-486.
43. Wong, C.-J., et al., *Longitudinal measures of RNA expression and disease activity in FSHD muscle biopsies.* Human molecular genetics, 2020. **29**(6): p. 1030-1043.
44. Heery, D.M., et al., *A signature motif in transcriptional co-activators mediates binding to nuclear receptors.* Nature, 1997. **387**(6634): p. 733-6.
45. Plevin, M.J., M.M. Mills, and M. Ikura, *The LxxLL motif: a multifunctional binding sequence in transcriptional regulation.* Trends Biochem Sci, 2005. **30**(2): p. 66-9.
46. Litterst CM. and P. E, *An LXXLL motif in the transactivation domain of STAT6 mediates recruitment of NCoA-1/SRC-1.* Journal of Biological Chemistry, 2002. **277**(39): p. 36052-36060.
47. Shuai, K. and B. Liu, *Regulation of gene-activation pathways by PIAS proteins in the immune system.* Nat Rev Immunol, 2005. **5**(8): p. 593-605.
48. Chung, C.D., et al., *Specific inhibition of Stat3 signal transduction by PIAS3.* Science, 1997. **278**(5344): p. 1803-5.
49. Liu, B., et al., *Inhibition of Stat1-mediated gene activation by PIAS1.* Proc Natl Acad Sci U S A, 1998. **95**(18): p. 10626-31.
50. Ungureanu, D., et al., *PIAS proteins promote SUMO-1 conjugation to STAT1.* Blood, 2003. **102**(9): p. 3311-3313.
51. Liu, B., et al., *A transcriptional corepressor of Stat1 with an essential LXXLL signature motif.* Proc Natl Acad Sci U S A, 2001. **98**(6): p. 3203-7.
52. Liu, B., et al., *Negative regulation of NF-kappaB signaling by PIAS1.* Mol Cell Biol, 2005. **25**(3): p. 1113-23.

53. Graham, C., et al., *The CIC-DUX4 fusion transcript is present in a subgroup of pediatric primitive round cell sarcomas.* Hum Pathol, 2012. **43**(2): p. 180-9.
54. Antonescu, C.R., et al., *Sarcomas With CIC-rearrangements Are a Distinct Pathologic Entity With Aggressive Outcome: A Clinicopathologic and Molecular Study of 115 Cases.* Am J Surg Pathol, 2017. **41**(7): p. 941-949.
55. Gambarotti, M., et al., *CIC–DUX4 fusion-positive round-cell sarcomas of soft tissue and bone: a single-institution morphological and molecular analysis of seven cases.* Histopathology, 2016. **69**(4): p. 624-634.
56. Brahmi, M., et al., *CIC-DUX4 sarcomas.* Current Opinion in Oncology, 2022. **34**(4): p. 342-347.
57. Nakai, S., et al., *Establishment of a novel human CIC-DUX4 sarcoma cell line, Kitra-SRS, with autocrine IGF-1R activation and metastatic potential to the lungs.* Sci Rep, 2019. **9**(1): p. 15812.
58. Lilljebjörn, H., et al., *Identification of ETV6-RUNX1-like and DUX4-rearranged subtypes in paediatric B-cell precursor acute lymphoblastic leukaemia.* Nature Communications, 2016. **7**(1): p. 11790.
59. Zhang, J., et al., *Deregulation of DUX4 and ERG in acute lymphoblastic leukemia.* Nat Genet, 2016. **48**(12): p. 1481-1489.
60. Rehn, J.A., et al., *DUX Hunting—Clinical Features and Diagnostic Challenges Associated with DUX4-Rearranged Leukaemia.* Cancers, 2020. **12**(10): p. 2815.
61. Snider, L., et al., *Facioscapulohumeral dystrophy: incomplete suppression of a retrotransposed gene.* PLoS Genet, 2010. **6**(10): p. e1001181.
62. Das, S. and B.P. Chadwick, *Influence of Repressive Histone and DNA Methylation upon D4Z4 Transcription in Non-Myogenic Cells.* PLoS One, 2016. **11**(7): p. e0160022.
63. Campbell, A.E., et al., *Facioscapulohumeral dystrophy: activating an early embryonic transcriptional program in human skeletal muscle.* Hum Mol Genet, 2018. **27**(R2): p. R153-R162.
64. Chew, G.L., et al., *DUX4 Suppresses MHC Class I to Promote Cancer Immune Evasion and Resistance to Checkpoint Blockade.* Dev Cell, 2019. **50**(5): p. 658-671 e7.
65. Jagannathan, S., et al., *Model systems of DUX4 expression recapitulate the transcriptional profile of FSHD cells.* Hum Mol Genet, 2016. **25**(20): p. 4419-4431.
66. Geng, L.N., A.E. Tyler, and S.J. Tapscott, *Immunodetection of human double homeobox 4.* Hybridoma (Larchmt), 2011. **30**(2): p. 125-30.
67. Wallace, L.M., et al., *DUX4, a candidate gene for facioscapulohumeral muscular dystrophy, causes p53-dependent myopathy in vivo.* Ann Neurol, 2011. **69**(3): p. 540-52.
68. Rosowski, E.E., et al., *Toxoplasma gondii Inhibits gamma interferon (IFN-gamma)- and IFN-beta-induced host cell STAT1 transcriptional activity by increasing the association of STAT1 with DNA.* Infect Immun, 2014. **82**(2): p. 706-19.
69. Kaya-Okur, H.S., et al., *CUT&Tag for efficient epigenomic profiling of small samples and single cells.* Nat Commun, 2019. **10**(1): p. 1930.
70. Rickard, A.M., L.M. Petek, and D.G. Miller, *Endogenous DUX4 expression in FSHD myotubes is sufficient to cause cell death and disrupts RNA splicing and cell migration pathways.* Hum Mol Genet, 2015. **24**(20): p. 5901-14.
71. Wen, Z., Z. Zhong, and J.E. Darnell, Jr., *Maximal activation of transcription by Stat1 and Stat3 requires both tyrosine and serine phosphorylation.* Cell, 1995. **82**(2): p. 241-50.

72. Sadzak, I., et al., *Recruitment of Stat1 to chromatin is required for interferon-induced serine phosphorylation of Stat1 transactivation domain.* Proc Natl Acad Sci U S A, 2008. **105**(26): p. 8944-9.
73. Savkur, R.S. and T.P. Burris, *The coactivator LXXLL nuclear receptor recognition motif.* J Pept Res, 2004. **63**(3): p. 207-12.
74. Kubota, T., et al., *PIASy inhibits virus-induced and interferon-stimulated transcription through distinct mechanisms.* J Biol Chem, 2011. **286**(10): p. 8165-8175.
75. Gross, M., et al., *Distinct effects of PIAS proteins on androgen-mediated gene activation in prostate cancer cells.* Oncogene, 2001. **20**(29): p. 3880-7.
76. Siatecka, M., et al., *Transcriptional activity of erythroid Kruppel-like factor (EKLF/KLF1) modulated by PIAS3 (protein inhibitor of activated STAT3).* J Biol Chem, 2015. **290**(15): p. 9929-40.
77. Mo, J., et al., *DDX3X: structure, physiologic functions and cancer.* Mol Cancer, 2021. **20**(1): p. 38.
78. Gu, L., et al., *Human DEAD box helicase 3 couples IkappaB kinase epsilon to interferon regulatory factor 3 activation.* Mol Cell Biol, 2013. **33**(10): p. 2004-15.
79. Schroder, M., M. Baran, and A.G. Bowie, *Viral targeting of DEAD box protein 3 reveals its role in TBK1/IKKepsilon-mediated IRF activation.* EMBO J, 2008. **27**(15): p. 2147-57.
80. Oshiumi, H., et al., *DEAD/H BOX 3 (DDX3) helicase binds the RIG-I adaptor IPS-1 to up-regulate IFN-beta-inducing potential.* Eur J Immunol, 2010. **40**(4): p. 940-8.
81. Ferguson, B.J., et al., *DNA-PK is a DNA sensor for IRF-3-dependent innate immunity.* Elife, 2012. **1**: p. e00047.
82. Shadle, S.C., et al., *DUX4-induced bidirectional HSATII satellite repeat transcripts form intranuclear double stranded RNA foci in human cell models of FSHD.* Hum Mol Genet, 2019.
83. Shadle, S.C., et al., *DUX4-induced dsRNA and MYC mRNA stabilization activate apoptotic pathways in human cell models of facioscapulohumeral dystrophy.* PLoS Genet, 2017. **13**(3): p. e1006658.
84. Maston, G.A., et al., *Non-canonical TAF complexes regulate active promoters in human embryonic stem cells.* Elife, 2012. **1**: p. e00068.
85. Bolger, A.M., M. Lohse, and B. Usadel, *Trimmomatic: a flexible trimmer for Illumina sequence data.* Bioinformatics, 2014. **30**(15): p. 2114-20.
86. Liao, Y., G.K. Smyth, and W. Shi, *The R package Rsubread is easier, faster, cheaper and better for alignment and quantification of RNA sequencing reads.* Nucleic Acids Res, 2019. **47**(8): p. e47.
87. Love, M.I., W. Huber, and S. Anders, *Moderated estimation of fold change and dispersion for RNA-seq data with DESeq2.* Genome Biol, 2014. **15**(12): p. 550.
88. Savan, R., et al., *Structural conservation of interferon gamma among vertebrates.* Cytokine Growth Factor Rev, 2009. **20**(2): p. 115-24.
89. Secombes, C.J. and J. Zou, *Evolution of Interferons and Interferon Receptors.* Frontiers in Immunology, 2017. **8**.
90. Shaw, A.E., et al., *Fundamental properties of the mammalian innate immune system revealed by multispecies comparison of type I interferon responses.* PLOS Biology, 2017. **15**(12): p. e2004086.

91. Saikruang, W., et al., *The RNA helicase DDX3 promotes IFNB transcription via enhancing IRF-3/p300 holocomplex binding to the IFNB promoter.* Scientific Reports, 2022. **12**(1): p. 3967.
92. Choi, H., et al., *Targeting DDX3X Triggers Antitumor Immunity via a dsRNA-Mediated Tumor-Intrinsic Type I Interferon Response.* Cancer Res, 2021. **81**(13): p. 3607-3620.
93. Resnick, R., et al., *DUX4-Induced Histone Variants H3.X and H3.Y Mark DUX4 Target Genes for Expression.* Cell Reports, 2019. **29**(7): p. 1812-1820.e5.